Geophysical Responses of Organic-rich Shale and the Effect of Mineralogy

---

A Thesis Presented to

the Faculty of the Department of Earth and Atmospheric Sciences

University of Houston

In Partial Fulfillment

of the Requirements for the Degree

Master of Science

By

Zhiwei Qian

May 2013

Geophysical Responses of Organic-rich Shale and the Effect of Mineralogy

Zhiwei Qian

APPROVED:

Dr. Dehua Han, Chairman
Department of Geosciences

Dr. Huawei Zhou
Department of Geosciences

Dr. Michael Murphy
Department of Geosciences

Dr. Enru Liu
ExxonMobil Upstream Research Company

Dean, College of Natural Science and Mathematics

ACKNOWLEDGEMENTS

I would like to thank my advisor Dr. Dehua Han and my committee members, Dr. Huawei Zhou, Dr. Michael Murphy, and Dr. Enru Liu for their guidance, valuable remarks, and corrections.

Dr. Han, my dissertation supervisor, has provided guidance and contributed many useful suggestions to this dissertation. I appreciate his patient instructions on this dissertation. I also want to thank Dr. Zhou, Dr. Murphy, and Dr. Liu for their useful comments, suggestions, and encouragement in my study. Special thanks extend to Luanxiao Zhao, Melleswel Yung, and Jianxiong Chen; the discussion with them inspires me a lot.

Geophysical Responses of Organic-rich Shale and the Effect of Mineralogy

---

An Abstract of a Thesis

Presented to

the Faculty of the Department of Earth and Atmospheric Sciences

University of Houston

In Partial Fulfillment

of the Requirements for the Degree

Master of Science

By

Zhiwei Qian

May 2013

ABSTRACT

Total organic carbon (TOC) is one of the most important parameters for indicating the resource potential of unconventional shale reservoirs. Because of the low density and velocity of organic matter, some seismic attributes like P-wave impedance (Ip) and Vp/Vs ratio would respond to high TOC content. So we can use these seismic attributes to remotely identify organic-rich areas.

However, these attributes are not equally efficient for all shale formations. The behavior of the geophysical response on TOC content may vary due to mineral variations of different shale plays. So, it is important to understand the mineral composition, study their impact on geophysical responses, and choose the right seismic attributes for the interpretation of a certain shale play. A rock physics modeling can be applied to link the in-situ rock parameters like mineral composition, TOC content, porosity etc. with the geophysical response.

In this thesis work, I study the geophysical response of Barnett shale. In addition, I study the impacts of the mineral variations within an individual shale reservoir on geophysical response. Certain relationships between TOC and volume percentage of clay and quartz were observed, which should be taken into account when performing rock physics modeling, as opposed to assuming the mineral composition changing randomly.

CONTENTS

Chapter 1 Introduction

1.1 Introduction of organic-rich shale

Shale is a fine-grained, detrital sedimentary rock that is by far the most abundant sedimentary rocks. The tiny grain size of shale indicates that it should deposit at quiet, non-turbulent environments like lakes, river floodplains, lagoons, swamps, and deep-ocean basins (Tarbuck et al., 2008).

The deposited clay and silt particles are randomly oriented at the beginning. However, as time goes by, the new sediments piled up on the previous ones would compact the previous ones and make them parallel to each other. During this process, the porosity of shale would be reduced dramatically and finally result in extremely low porosity and permeability.

If there is organic material deposited and preserved, the shale could become organic-rich source rocks. After being deeply buried and properly heated, the organic matter would produce oil and gas. The high pressure caused by volume expansion from solid to liquid, and liquid to gas during this process would induce micro-fractures; the produced hydrocarbons would then be released though these micro-fractures into carrier systems and finally conventional reservoir. The pressure in the source rock would decline after the expulsion of hydrocarbons, and then the micro-fractures would heal (Figure1-1).

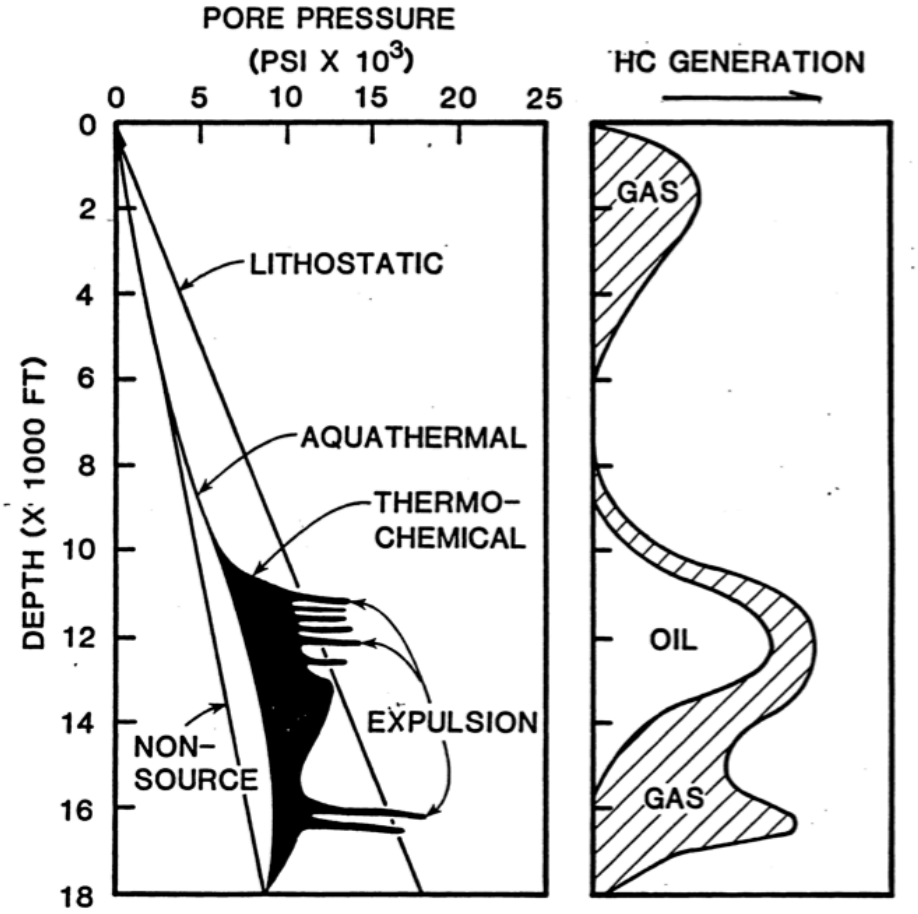

(Bissada, 1994)

Figure 1-1: The generation of hydrocarbon would increase the pore pressure because of volume expansion form solid to liquid to gas. When the pore pressure exceeds the litho-static pressure, the pressure-induced micro-fracture would release the produced hydrocarbons. The excessive pressure would be released after that. We can see from the picture that the expulsion process is not continuous. The releasing process is more like pulses because it would take a long time to produce a little bit hydrocarbons.

Conventionally, shale is only considered as seal rock because of its low permeability.

However, only recently, organic-rich shale is considered as a resource:

1: The organic matter itself is very porous. Part of the generated hydrocarbons would be sucked inside the organic matter just like water being absorbed in sponge.

2: The expulsion of hydrocarbons requires the generation of excessive pore pressure

to induce fracture in the source shale, which means, if the pore pressure threshold is not reached, the produced hydrocarbons would stay inside the source shale instead of being expulsed to conventional reservoirs.

3: The development of horizontal drilling and hydraulic fracturing makes it possible to commercially exploit the hydrocarbons in the low permeable organic-rich shale.

1.2 Importance of organic matter

The United States unconventional oil and gas outlook (Figure 1-2) shows the production capacity of unconventional resource. As a kind of unconventional resource, the production capacity of shale has increased continuously during the past 20 years, and has increasing potential in the future. Therefore, industry and research institute are paying more and more attention on organic-rich shale.

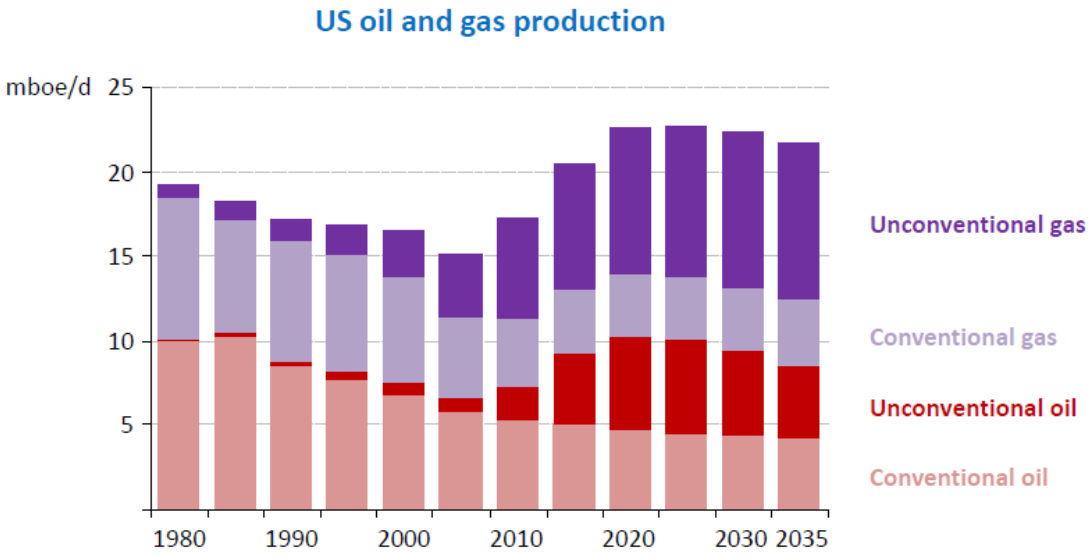

Figure 1-2, Energy outlook 2012 (from IEA)

The production capacity of unconventional source increase continuously

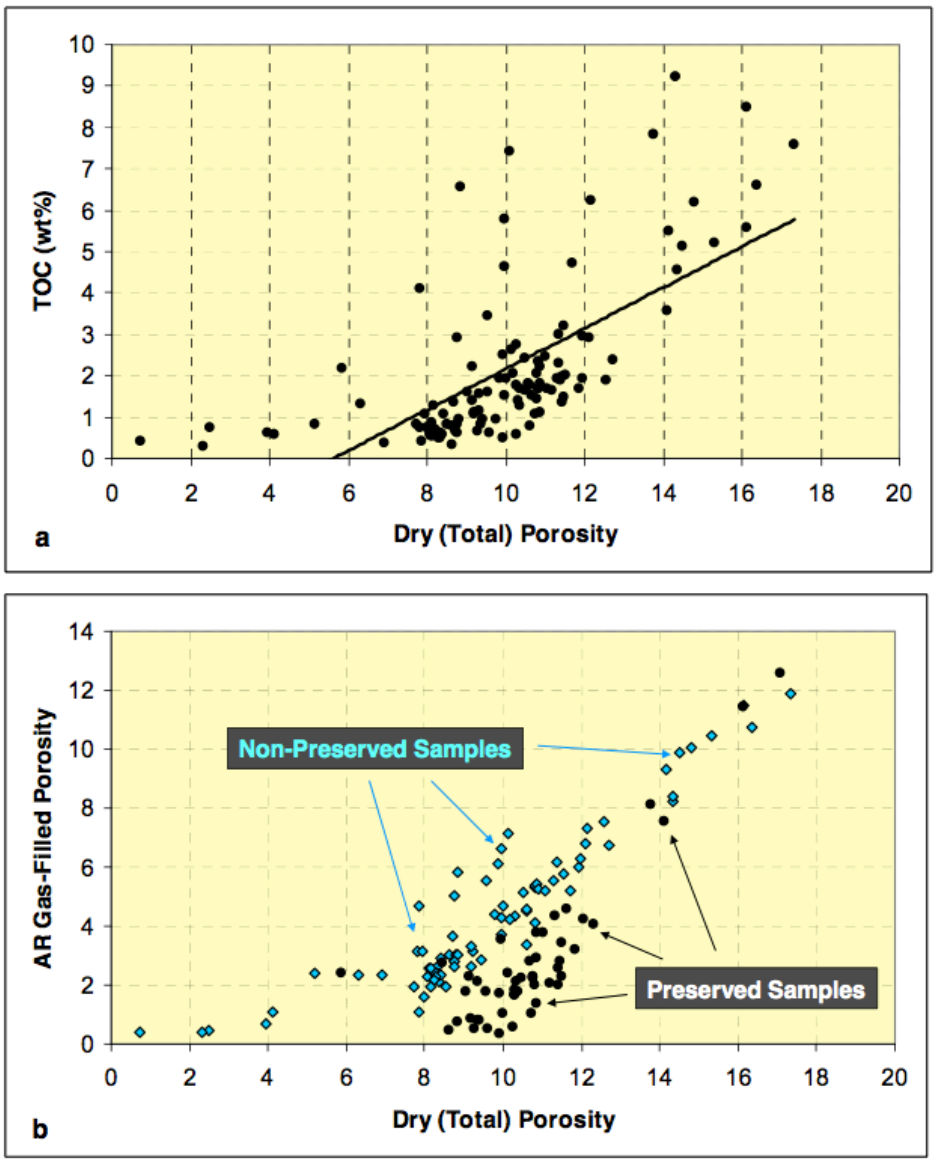

Figure 1-3 a) Relation between Total Porosity (p.u.) and TOC (wt%); b) relation between Total Porosity (p.u.) and As-Received Gas-Filled Porosity (p.u.) for preserved and non-preserved samples. Preserved samples are recommended. (Passey et al., 2010)

Organic enrichment is one of the most important parameters for shale play.

First, it indicates the oil and gas generation potential. For example, Figure 1-3 shows the total porosity and gas content (gas-filled porosity or bulk-volume gas BVG) are directly associated with the TOC content of the rock (TOC is a measurement of organic enrichment, which would be explained later). That means high local TOC is a

critical factor to assess when evaluating potential shale-gas reservoirs (Passey et al., 2010).

Secondly, as mentioned in section 1.1, the porosity of organic matter is high. After the generation of hydrocarbons, some of them is not able to overcome the retention capacity of the organic matter and therefore is sucked inside the pores of organic matter. So organic-enriched source rocks can also be considered as special reservoirs.

Finally, we can start to heat immature organic matters to produce hydrocarbons. The Shell started an In-situ Conversion Process (ICP) in Colorado since 1980 (Bartis et al., 2005). They heat oil shale at approximately 650°F to convert organic matter into oil and gas (Lee et al., 2007). Although some energy would be consumed to heat the oil shale, the whole program is still commercially meaningful because we can use cheaper energy like gas, which is hard to store and transport, to trade for more expensive energy like oil.

1.3 Evaluation of organic enrichment

The organic enrichment can be quantified by total organic carbon (TOC), which can be measured in laboratory using combustion method. Since TOC measured both reactive organic matter and dead carbon, it cannot tell the real hydrocarbon generation potential by itself. For example, an over-matured sample could also have high TOC even though its hydrocarbon has been totally burned out by heat. So we need a new parameter that can measure total hydrocarbon generation potential (THGP). Rock-Eval Pyrolysis process can be used to measure this parameter.

However, THGP only indicates the potential, but cannot ensure high productivity. Shallow, young sediments usually will not generate commercially meaningful hydrocarbons (except marsh gas) even with high THGP. As time passing by, the young sediments being buried deeper and deeper, the ambient temperature would increase because of the geothermal gradient. Increasing temperature keeps cooking kerogen in the rock, making them matured and turned into oil and gas. The hydrocarbon generation processes are divided into five stages based on maturation level, as shown in Figure 1-4. Usually zone III is considered as the primary production zone of oil and gas. If the whole process does not stop at this time, the source rock would pass the perfect oil, gas generation window and become over-matured. Finally, under extremely high temperature and long cooking time, all hydrocarbons would be burned out and the only thing left would be dead carbon.

The type of organic matter is also an important parameter. If the organic matter is type III gas-prone source, we would only get small amount of oil.

Even if all the above parameters say high productivity, we still cannot ensure the exploitation of economically meaningful amount of hydrocarbons. To conduct hydraulic fracturing on low permeable shale, we need to investigate the mineralogy of the source rock to estimate its brittleness, and understand the stress field to estimate fracture pattern. Hydrocarbon exploration is complicated. In this thesis I would only focus on the estimation of TOC.

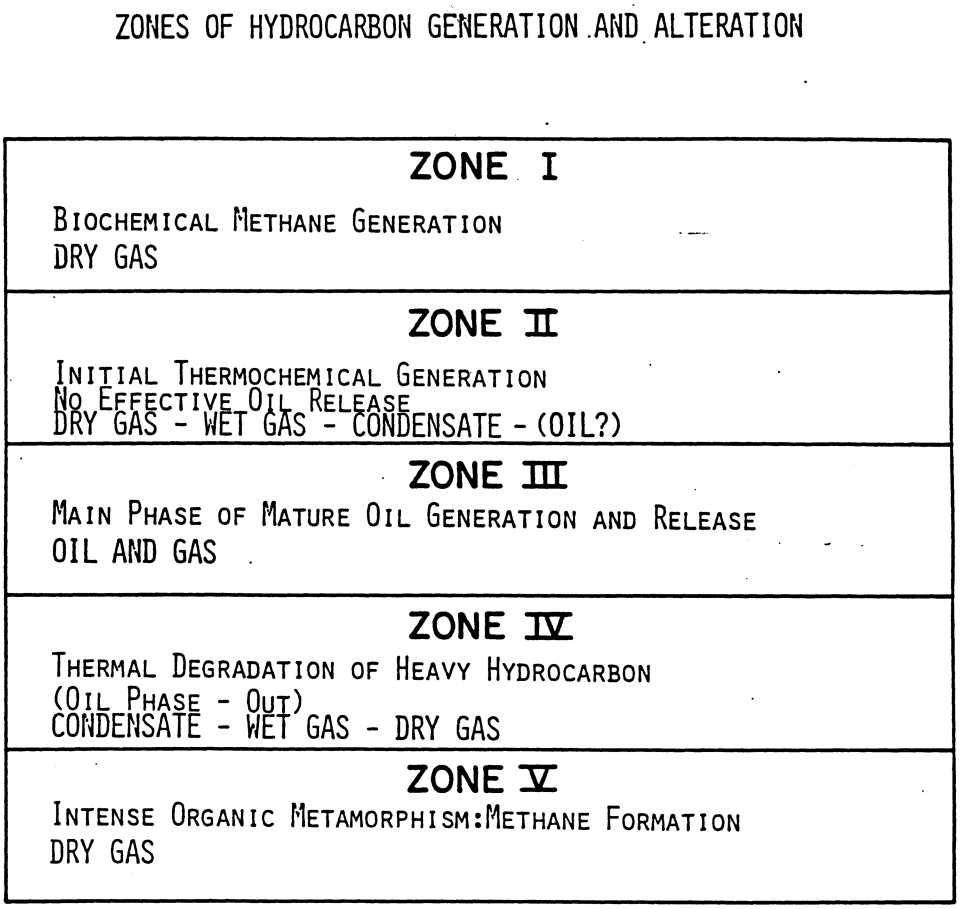

(Bissada, 1994)

Figure 1-4, Zones of hydrocarbon generation and alteration

1.4 Motivation

If core samples are available, we can directly measure the TOC (and other useful parameters like THGP, maturation level, etc.) in laboratory. However, core samples are always expensive and difficult to get. The lateral and vertical heterogeneity of shale reservoirs makes it insufficient to characterize the whole shale reservoir using limited core samples.

Geophysical methods can remotely detect organic-rich spots. Using a rock physics modeling, we can link the in-situ rock parameters like mineral composition, TOC

content, porosity etc. with the geophysical response. After the success of forward modeling, we can inversely estimate the rock properties (including TOC content) from well log and seismic data (Zhu et al., 2011).

Because of the low density and velocity of organic matter, seismic attributes like Ip and Vp/Vs would respond to high TOC content. However, these attributes are not equally efficient for all shale formation. The behavior of the geophysical response on increasing TOC content may vary due to the different mineralogy of different shale play (Zhu et al, 2011).

The motivations of this thesis work are (1): Study the effects of different in-situ rock parameters on geophysical response; (2): Find out the optimum kerogen identification seismic attributes for Barnett shale (a case study); and (3): Improve the rock physics modeling by taking the relationships between the kerogen and clay content and the kerogen and quartz content into account.

1.5 Overview of thesis

This study is divided into five parts. Chapter 2 describes different methods to estimate TOC value. In Chapter 3 I introduce rock physics modeling aim at predicting the effect of kerogen, mineralogy and porosity on geophysical response using rock physics modeling. In Chapter 4 I discuss the impacts of mineralogy in detail. Chapter 5 is summary of the thesis.

Chapter 2 TOC estimation methods

2.1 Laboratory analyses:

The method to estimate Total Organic Carbon (TOC) in laboratory is introduced. Usually, rock samples would contain both inorganic carbon and organic carbon. We want to estimate organic carbon only, so the first step it to remove inorganic carbon. We acidify the samples to dissolve its inorganic carbon and release the produced gas into air. Then the next step is to let the samples go through a high-temperature (1,350 °C) combustion process to oxidize the remaining organic carbon into carbon dioxide. The produced gas would be measured to estimate TOC value (Bissada, 1994).

However, as mentioned in Chapter 1, shale reservoirs are extremely heterogeneous vertically and laterally. This makes the limited number of core samples insufficient. So other TOC estimation methods like well log and seismic methods are needed.

2.2 Well log analyses:

Because of its special properties, organic matter would give rise to special well log response. Therefore, we can use well log data to estimate the amount of organic matter.

Gamma ray

Some organic matters contain uranium, resulting in high gamma-ray value (Beers, 1945; Swanson, 1960). However, uranium in organic matter is not the only thing that

can cause high gamma-ray value. Thorium in clay minerals and potassium in feldspar are also responsible for high gamma ray value. So we need to break the total gamma ray counts into three components: uranium, potassium and thorium for better TOC prediction, as shown in Figure2-1. However, for those organic matters contain less uranium than others, this gamma-ray method would underestimate the organic matter content (Schmoker, 1981; Supernaw et al., 1978; Fertl and Rieke, 1980).

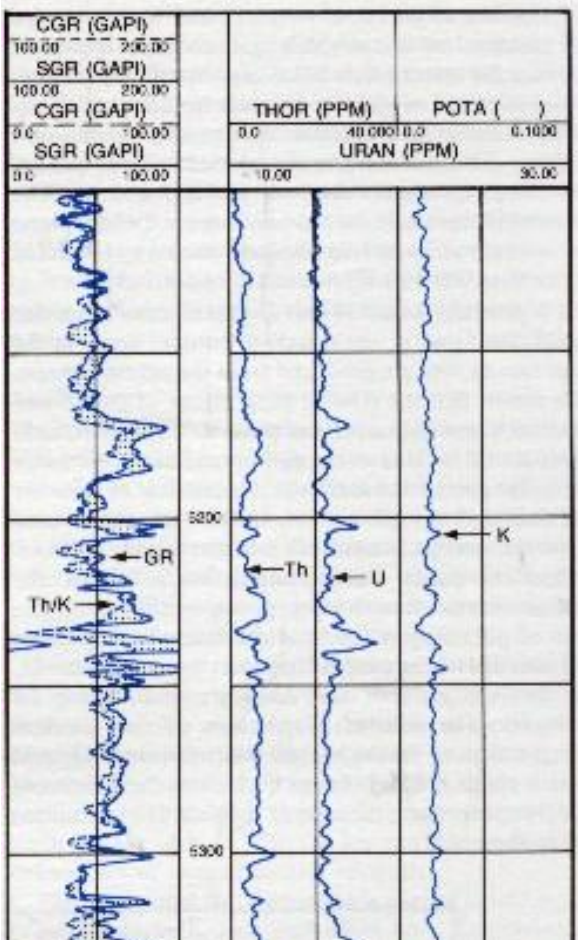

Figure 2-1 Gamma ray (track 1) and its three component(track 2 and 3) (Schlumberger)

Density log

Because rock matrix is denser than solid organic matter, density log has smaller

reading in the intervals containing organic matter. However, many factors other than organic matter would affect density log reading. For example, high matrix porosity result in smaller density log reading; existence of heavy minerals like pyrite will balance low density value caused by organic matter and there will be no density log response even when TOC is high (Schmoker et al., 1983).

Resistivity log

The resistivity of oil and gas is very high compared with brine; therefore we can observe high resistivity log reading in source rock with matured organic carbon. This method cannot detect immature organic matter even when TOC and THGP are high (Meissner, 1978; Schmoker et al., 1989; Nixon, 1973).

Δ log R

In water-saturated non-source rocks, porosity log and resistivity log should parallel to each other if they are properly scaled, because water saturation in porous rocks reduce the resistivity. For organic-rich source rocks or hydrocarbon-saturated reservoir rocks, however, there will be a separation between these two curves. This separation, Δ log R, can be used to estimate the TOC of the rock（Passey et al., 1990.）

2.3 Geophysical analyses using well log/seismic data

We can also use geophysical method to identify organic-rich sweet spots.

Using rock physics modeling, we can link the in-situ rock parameters like mineral composition, TOC, porosity etc. with velocity, density, and other elastic parameters (Figure2-2). Using forward modeling process, we can study the effect of different

in-situ parameters on elastic parameters. We can inversely estimate important productivity-related in-situ parameters like TOC from elastic parameters. Elastic parameters can be either acquired from well log measurement or inverted form seismic data (Zhu et al., 2011).

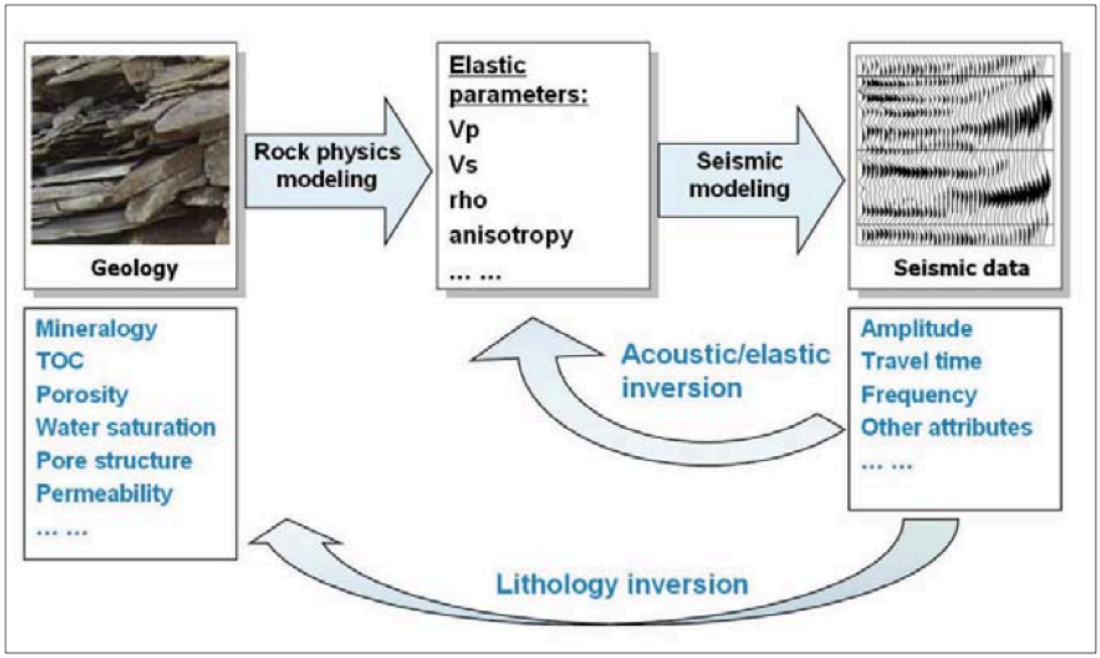

Figure 2-2 rock physics and seismic modeling/inversion workflow (Zhu et al., 2011)

Chapter 3 Rock physics modeling

3.1 Effective medium theory

Theoretical estimation of the effective moduli of mixed grains and pores generally depends on the volume fractions of the various phases, the properties of the individual components of the composite, the geometric details of the shapes, and spatial distributions of the components. If we specify only the volume fractions and the constituent moduli, the best we can do is to predict the upper and lower bounds. Voigt and Reuss bounds are the simplest bounds. At any given volume fraction of constituents the effective modulus will fall between the bounds, but its precise value depends on the geometric details (Mavko et al., 2009).

If specific inclusion shapes are assumed, we can then obtain effective moduli. Self-consistent approximation is one of many methods of this kind of estimations.

Voigt and Reuss bounds

Voigt and Reuss bounds provide a fundamental model for iso-strain and iso-stress conditions.

Voigt upper bound of the effective elastic modulus, M_V, of N phases is

$$Mv = \sum_{i=1}^{N} f_i M_i$$

Where f_i is the volume fraction of the ith phase and M_i is the elastic modulus of the ith phase (Mavko et al., 2009).

A sketch of the geometry of Voigt bound is shown on Figure 3-1. We call it iso-strain

because the stiffer components of the composite sustain most of the stress therefore all constituents have the same strain under ideal condition. Voigt upper bound describes the behaviors of some artificial structures like building; few natural rocks can reach the Voigt bound.

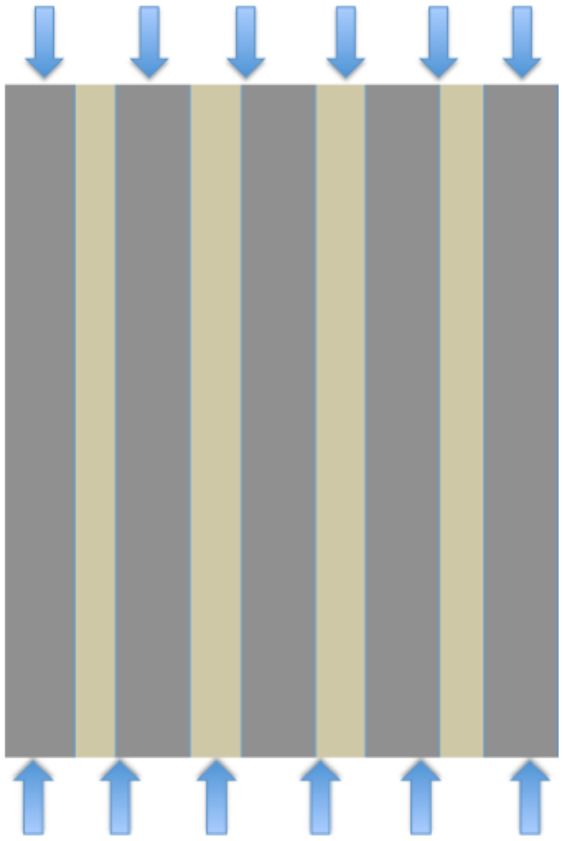

Figure 3-1 Geometry of Voigt bound, all constituents have the same strain. So it is called the iso-strain average.

Reuss lower bound of the effective elastic modulus, M_R, of N phases is

$$\frac{1}{M_R} = \sum_{i=1}^{N} \frac{f_i}{M_i}$$

Where f_i is the volume fraction of the ith phase and M_i is the elastic modulus of the ith phase (Mavko et al., 2009).

A sketch of the geometry of Reuss bound is shown on Figure 3-2. We call it iso-stress because all constituents sustain the same stress and the softer constituent has more strain. Reuss lower bound describes the behaviors of several real rocks. When all constituents are gases and/or liquids, with zero shear moduli, the Reuss average gives the effective moduli of the mixture exactly (Mavko et al., 2009).

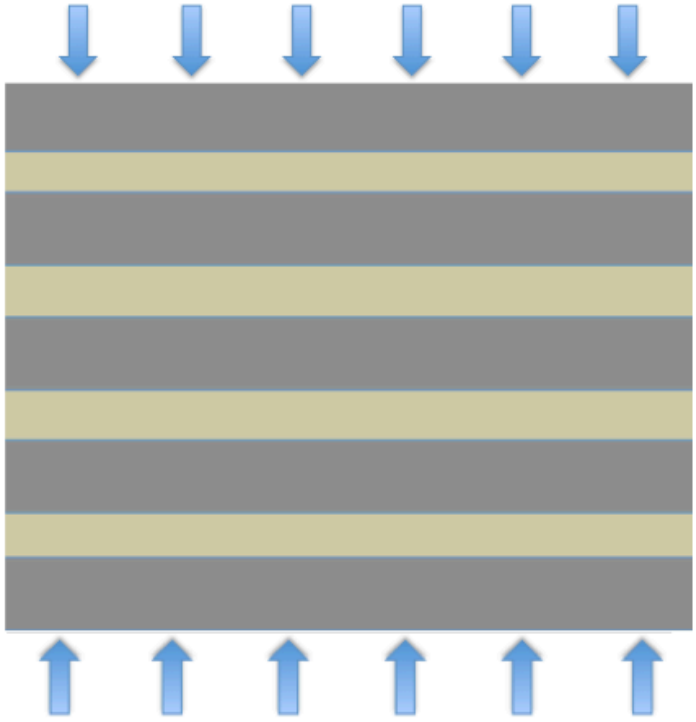

Figure 3-2 Geometry of Reuss bound, all constituents have the same stress. So it is called the iso-stress average.

Voigt-Reuss-Hill

Voigh-Reuss-Hill average is the arithmetic average of Voigt upper bound and Reuss lower bound:

$$M_{VRH} = \frac{M_V + M_R}{2}$$

It can be used to estimate the moduli of mixture.

Self-consistent approximations of effective moduli (SCA):

Most effective elastic theories are limited to dilute concentrations of the inclusions (Mavko et al., 2009). Self-consistent approximation method (Budiansky, 1965; Hill, 1965; Wu, 1966; Berryman, 1980) was proposed for higher concentrations. This method embeds the inclusions into a medium whose parameters are variable, then we adjust the embedding medium until the net scattering from inclusions vanishes identically (Berryman, 1980).

Berryman (1980, 1995) gives a general form of the self-consistent approximations for N-phase composites:

$$\sum_{i=1}^{N} x_i (K_i - K_{SC}^*)\, P^{*i} = 0$$

$$\sum_{i=1}^{N} x_i (\mu_i - \mu_{SC}^*)\, Q^{*i} = 0$$

i refers to the ith material, x_i is volume fraction of ith material, P and Q are geometric factors. For ellipsoidal inclusions of arbitrary aspect ratio, the coefficients P and Q are given by

$$P = \frac{1}{3} T_{iijj}$$

$$Q = \frac{1}{5}(T_{ijij} - \frac{1}{3} T_{iijj})$$

where

$$T_{iijj} = \frac{3F_1}{F_2}$$

$$T_{ijij} - \frac{1}{3}T_{iijj} = \frac{2}{F_3} + \frac{1}{F_4} + \frac{F_4F_5 + F_6F_7 - F_8F_9}{F_2F_4}$$

$$F_1 = 1 + A[\frac{3}{2}(f + \theta) - R(\frac{3}{2}f + \frac{5}{2}\theta - \frac{4}{3})]$$

$$F_2 = 1 + A\left[1 + \frac{3}{2}(f + \theta) - \frac{1}{2}R(3f + 5\theta)\right] + B(3 - 4R) +$$

$$\frac{1}{2}A(A + 3B)(3 - 4R)[f + \theta - R(f - \theta + 2\theta^2)]$$

$$F_3 = 1 + A\left[1 - \left(f + \frac{3}{2}\theta\right) + R(f + \theta)\right]$$

$$F_4 = 1 + \frac{1}{4}A[f + 3\theta + R(f - \theta)]$$

$$F_5 = A\left[-f + R\left(f + \theta - \frac{4}{3}\right)\right] + B\theta(3 - 4R)$$

$$F_6 = 1 + A[1 + f - R(f + \theta)] + B(1 - \theta)(3 - 4R)$$

$$F_7 = 2 + \frac{1}{4}A[3f + 9\theta - R(3f + 5\theta)] + B\theta(3 - 4R)$$

$$F_8 = A\left[1 - 2R + \frac{1}{2}f(R - 1) + \frac{1}{2}\theta(5R - 3)\right] + B(1 - \theta)(3 - 4R)$$

$$F_9 = A[(R - 1)f - R\theta] + B\theta(3 - 4R)$$

$$A = \frac{\mu_i}{\mu_m} - 1$$

$$B = \frac{1}{3}(\frac{K_i}{K_m} - \frac{\mu_i}{\mu_m})$$

$$R = \frac{(1 - 2\nu_m)}{2(1 - \nu_m)}$$

$$when\ \alpha > 1\ \theta = \frac{\alpha}{(\alpha^2 - 1)^{3/2}}[\alpha(\alpha^2 - 1)^{\frac{1}{2}} - cosh^{-1}\alpha]$$

$$when\ \alpha < 1\ \theta = \frac{\alpha}{(1-\alpha^2)^{3/2}}[cos^{-1}\alpha - \alpha(\alpha^2-1)^{\frac{1}{2}}]$$

$$f = \frac{\alpha^2}{1-\alpha^2}[3\theta - 2]$$

3.2 The effect of organic matter on the geophysical response

To study the effect of organic matter on the geophysical response of organic-rich shale, I built a simple rock physics model composed of kerogen and clay. A schematic illustration of the model is shown in Figure 3-3. The properties of the two end members are shown in Table 3-1.

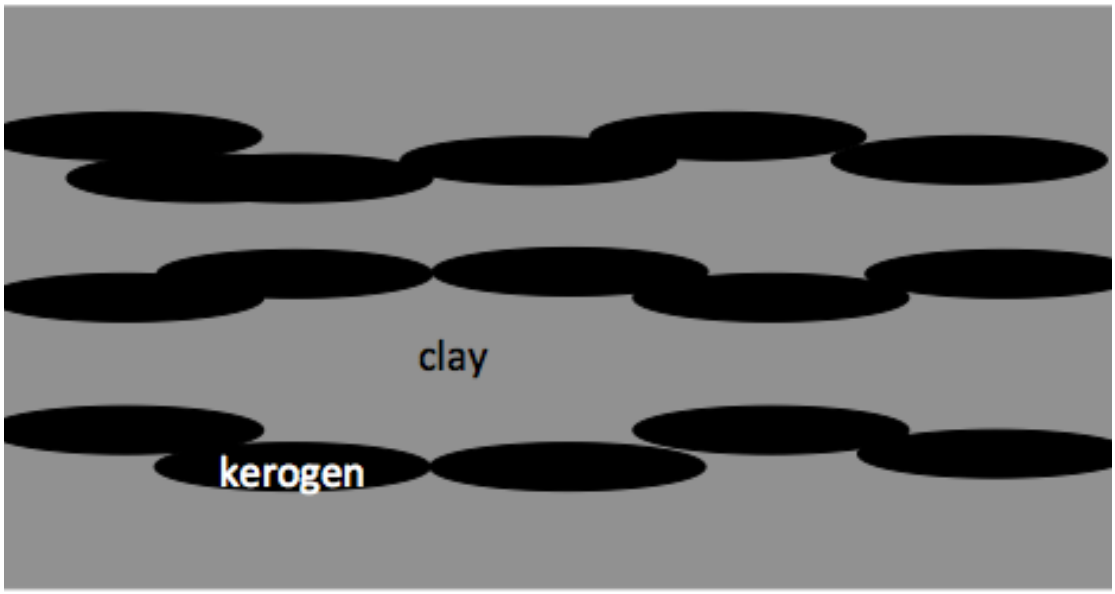

Figure 3-3 Simple rock physics model

	Bulk modulus K (Gpa)	Shear modulus MU (Gpa)	Density Rho (g/cm3)
Clay(1)	25	9	2.55
Kerogen(2)	5	2.5	1.2

Table 3-1 The bulk moduli, shear moduli and density of clay and kerogen, which is the two end members of the simple model. ((1)Han et al.1986; (2)RPL measured data)

If clay minerals are surrounded by kerogen, or if clay and kerogen have layered structure, the two constituents can be assumed to have the same stress. Therefore, their effective moduli should be close to Reuss bound prediction. If kerogen embedded in stiff pores surrounded by clay, however, the effective moduli of the two constituents should be close to Voigt bound. Because the exact structure of the clay-kerogen system is unknown, I show both Reuss and Voigt bounds. Voigt-Reuss-Hill average is used to estimate the effective properties. After making simple assumption about the geometry of clay and kerogen (aspect ratio of clay = 0.1; aspect ratio of kerogen = 0.01), the SCA is used to predicted elastic properties.

The calculated effective bulk and shear moduli of this simple model using Voigt-Reuss bounds, Voigt-Reuss-Hill average and Self-consistent Approximation are shown in Figure 3-4. They are represented by blue, green, black, and red curve respectively. X-axis is the volume concentration of organic matter, Y-axis is the bulk and shear moduli. We can see that the elastic moduli predicted by SCA and Voigt-Reuss-Hill lie between the Voigt and Reuss bound, and both the bulk and shear moduli decrease with increasing kerogen content. This is because kerogen is a relatively softer material compared with the ambient rock. However, it is not a fluid, so it's shear moduli is not zero.

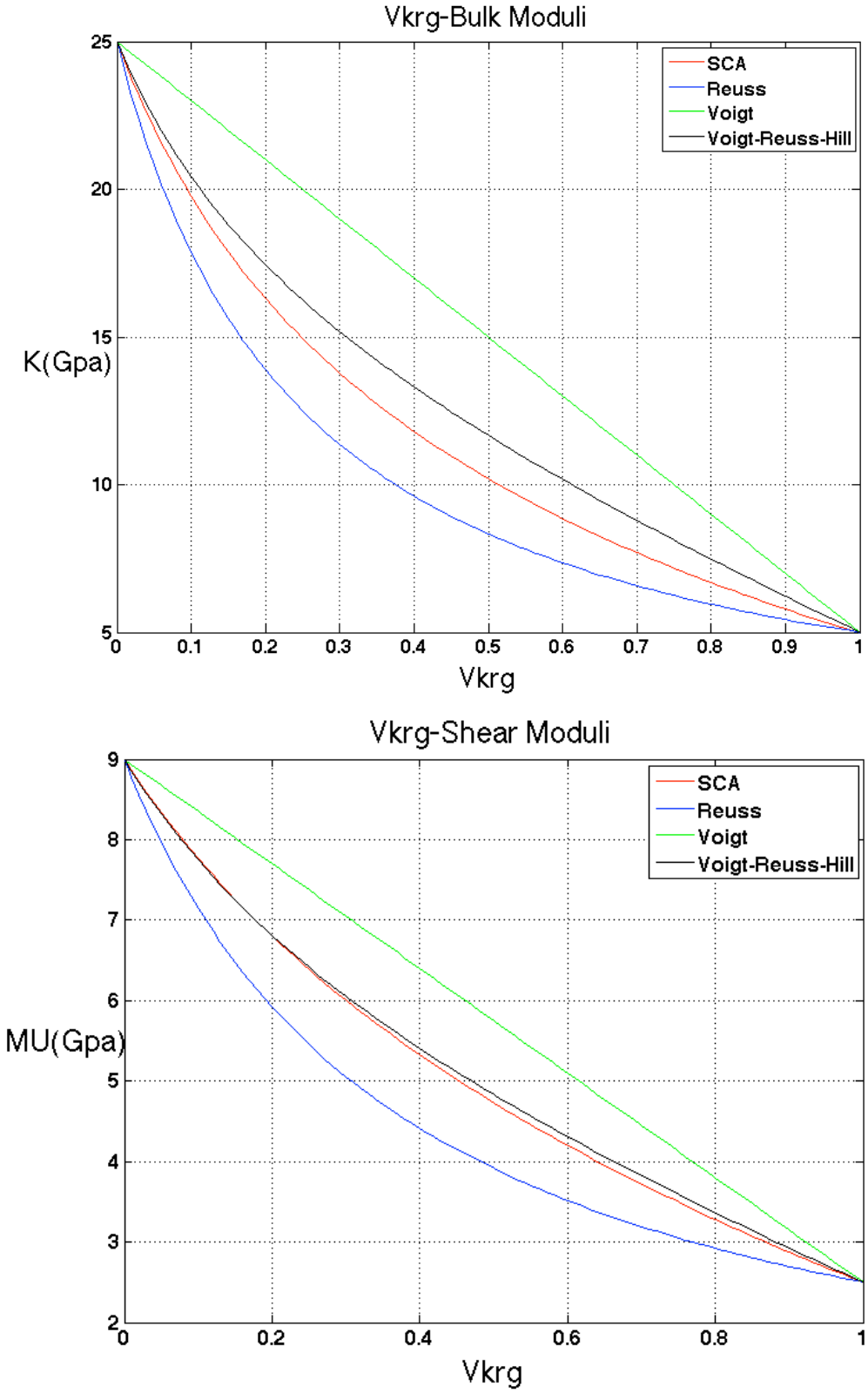

Figure 3-4 Effective bulk and shear moduli of the clay-kerogen model. The elastic moduli predicted by SCA and Voigt-Reuss-Hill lie between the Voigt and Reuss bound, and both the bulk and shear moduli decrease with increasing kerogen content.

Because

$$V_p = \sqrt{\frac{K + \frac{4}{3}\mu}{\rho}}$$

The effective P-wave impedance Ip are calculated by:

$$I_p = \rho * V_p = \sqrt{\rho * (K + \frac{4}{3}\mu)}$$

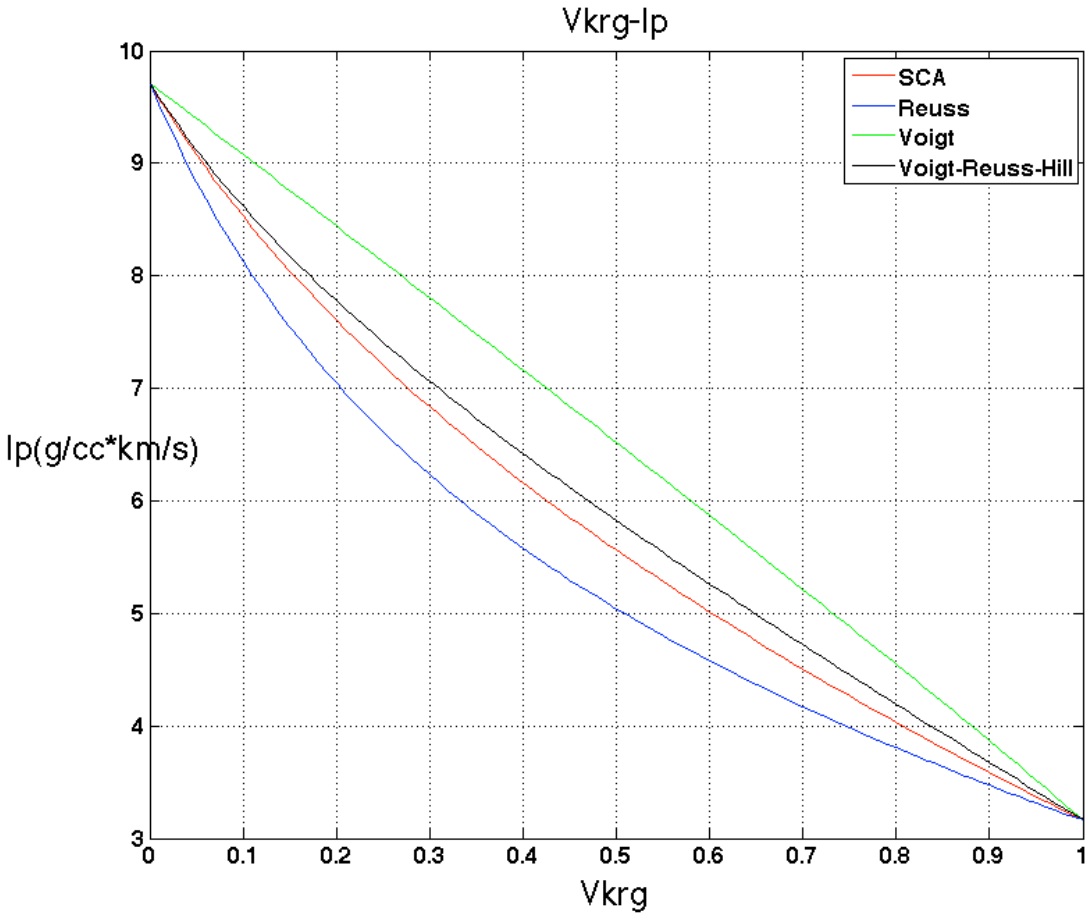

Figure 3-5: Model predicted relationship between P-wave impedance and the volume concentration of organic matter. P-wave impedance decreases as the volume concentration of organic matter increases.

Figure 3-5 shows the model predicted relationship between P-wave impedance and the volume concentration of organic matter.

We can see that P-wave impedance decreases as the volume concentration of organic matter increases. The main reason for such a TOC response is that organic matter has relatively lower density and P-wave velocity, therefore lower impedance than the matrix rock.

Because

$$V_s = \sqrt{\mu/\rho}$$

the effective Vp/Vs ratio is calculated by

$$\frac{V_p}{V_s} = \sqrt{\frac{K}{\mu} + \frac{4}{3}}$$

Figure 3-6 shows the model predicted relationship between Vp/Vs and the volume concentration of organic matter.

We can see that Vp/Vs ratio decreases as the volume concentration of organic matter increases. The main reason for such a TOC response is that organic matter has relatively lower Vp/Vs than the matrix (clay).

So in conclusion, for a clay-kerogen system, the effective K, Mu, Ip and Vp/Vs would all decrease with increasing kerogen content.

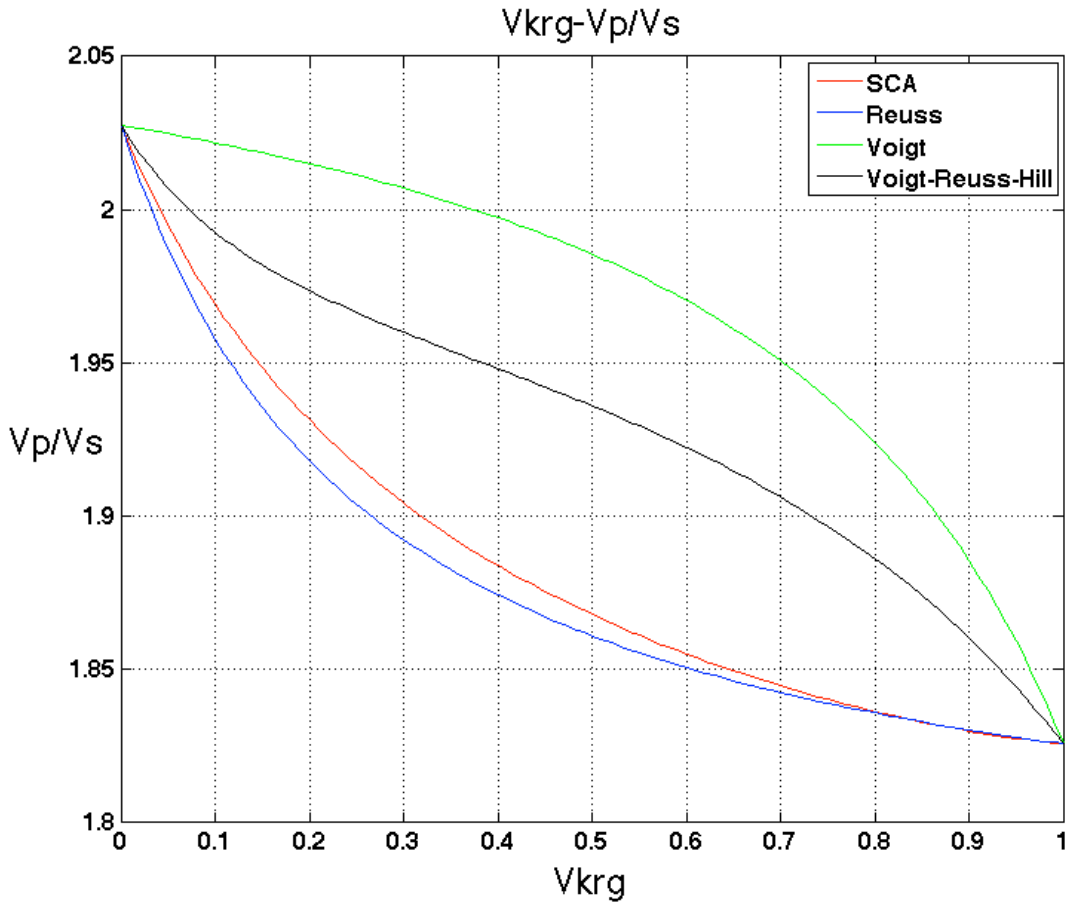

Figure 3-6 The model predicted relationship between Vp/Vs and the volume concentration of organic matter. Vp/Vs ratio decreases as the volume concentration of organic matter increases.

3.3 The effect of mineralogy

In the previous rock physics modeling process (section 3.2), I have assumed a clay-kerogen system. However, other factors like mineral composition, porosity and pore shape also have strong influences on the effective elastic property. I will discuss the effect of mineralogy first. I build a new model composed of clay and quartz. The properties of the two end members are shown in Table 3-2.

	Bulk modulus K (Gpa)	Shear modulus MU (Gpa)	Density Rho (g/cm3)
Clay(1)	25	9	2.55
Quartz(2)	37	44	2.65

Table 3-2 The bulk moduli, shear moduli and density of clay and quartz, which is the two end members of the simple model. ((1)Han et al.1986; (2) Mavko, 2009)

I calculate the effective bulk and shear moduli of this simple model using Voigt-Reuss bound, Voigt-Reuss-Hill average and Self-consistent Approximation, (Figure 3-7) which is represented by blue, green, black, and red curves respectively. X-axes is volume concentration of quartz, Y-axes is bulk and shear modulus. We can see that both the bulk and shear moduli increase with increasing quartz content.

The model predicted relationship between P-wave impedance, Vp/Vs ratio, and quartz content are shown in Figures 3-8 and 3-9, respectively. As shown in figures, for a quartz-clay system, the effect of increasing quartz is to increase P-wave impedance and decrease Vp/Vs.

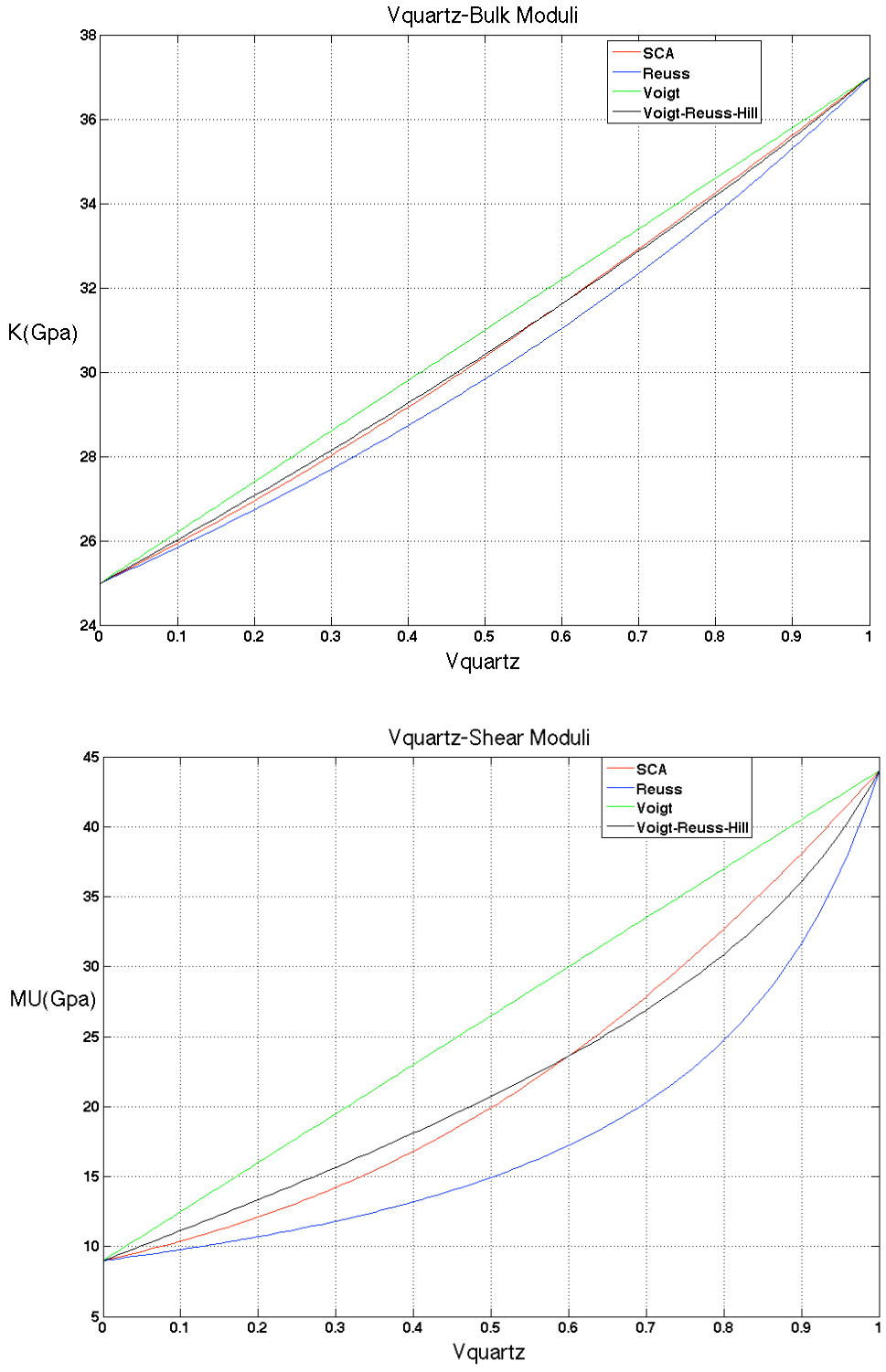

Figure 3-7 Effective bulk and shear moduli of a clay-quartz system. The elastic moduli predicted by SCA and Voigt-Reuss-Hill lie between the Voigt and Reuss bound, and both the bulk and shear moduli increase with increasing quartz content.

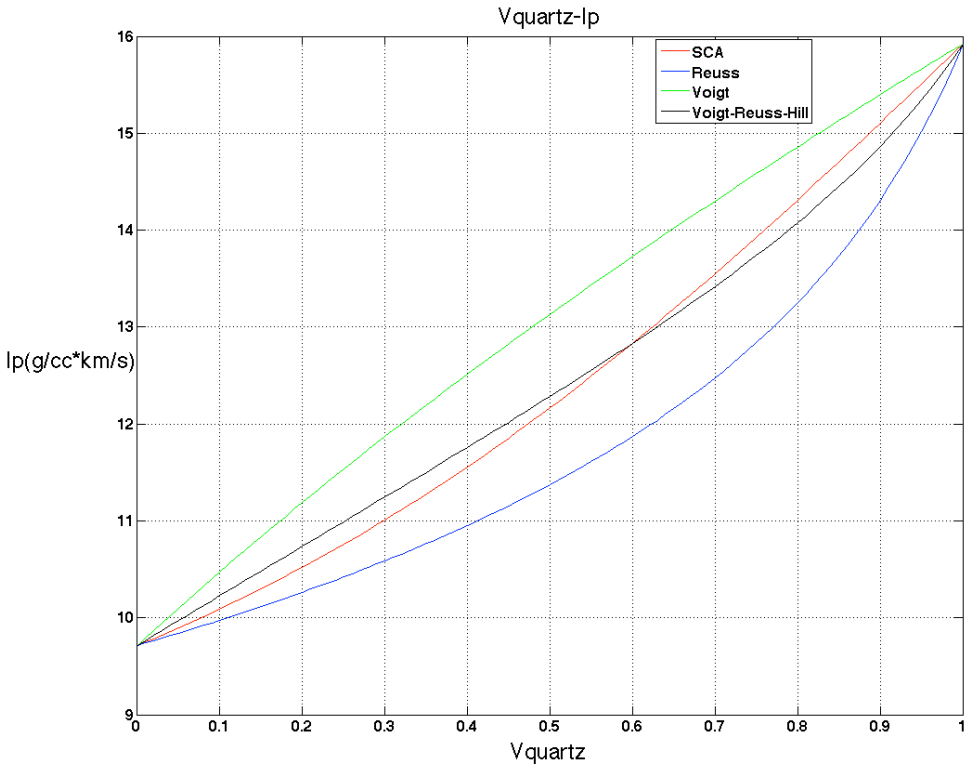

Figure 3-8 Model predicted relationship between P-wave impedance and the volume concentration of quartz. P-wave impedance increase as quartz content increase.

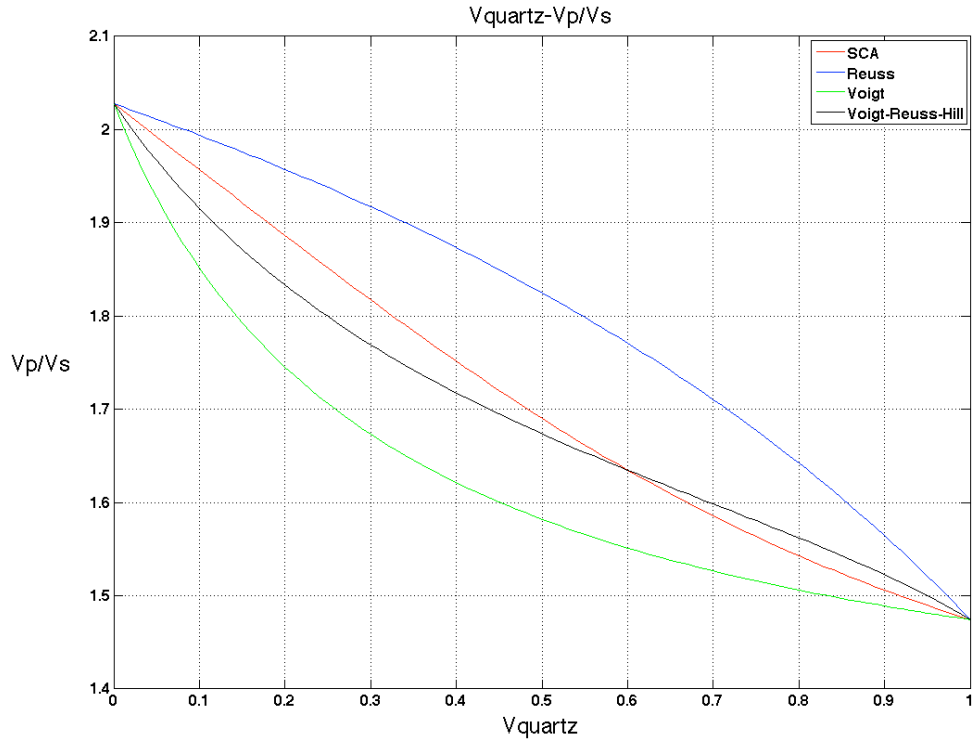

Figure 3-9 Model predicted relationship between Vp/Vs quartz content. Vp/Vs ratio decrease as quartz content increase.

3.4 The effects of porosity, pore shape and saturation

For organic-rich shale, there are inter-granular pores between clay minerals, they are compliant and have small aspect ratio. There are also micro-pores inside organic matter; they have higher aspect ratio therefore stiffer (Figure 3-10).

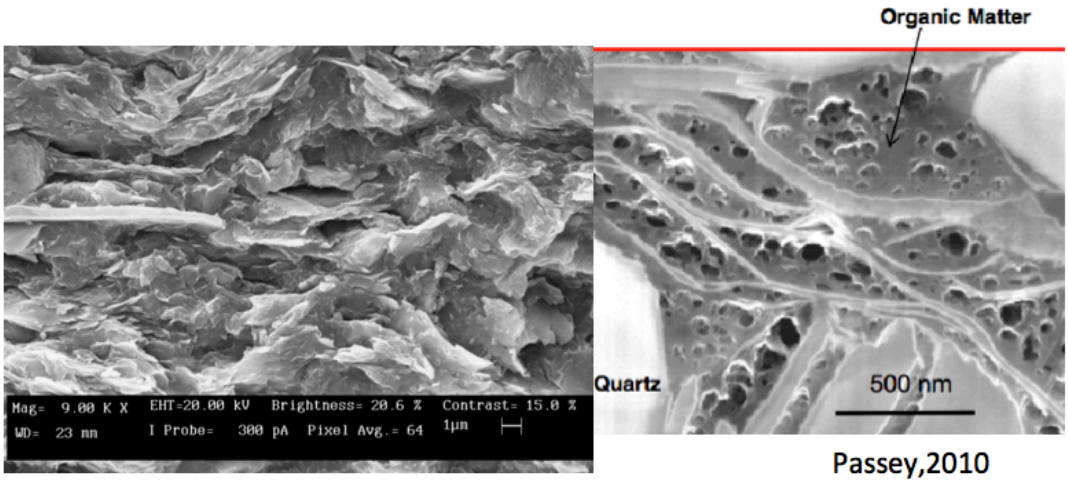

Figure 3-10 Flat pores between clay minerals with small aspect ratio (left) and micro-pores inside organic matter with higher aspect ratio (right).

I built a new model to take into account the effects of pores and minerals.

The model is composed of clay, quartz, kerogen (volume of kerogen is 10%), and 100% water saturated pores (aspect ratio = 0.4). Volume of quartz change from 50%-70%, and porosity change from 0%--9%.

Ip and Vp/Vs values shown in Figure 3-11 are calculated from SCA predicted effective elastic bulk and shear moduli of this model. X-axis is P-wave impedance and Y-axis is Vp/Vs ratio. The blue color represent low quartz percentage, and the red color represents high quartz percentage.

We can see that as quartz increases from 50% to 70%, the Vp/Vs ratio decreases, and

the Ip increases. As the porosity increases from 0% to 9%, the Ip decreases while no obvious change on Vp/Vs.

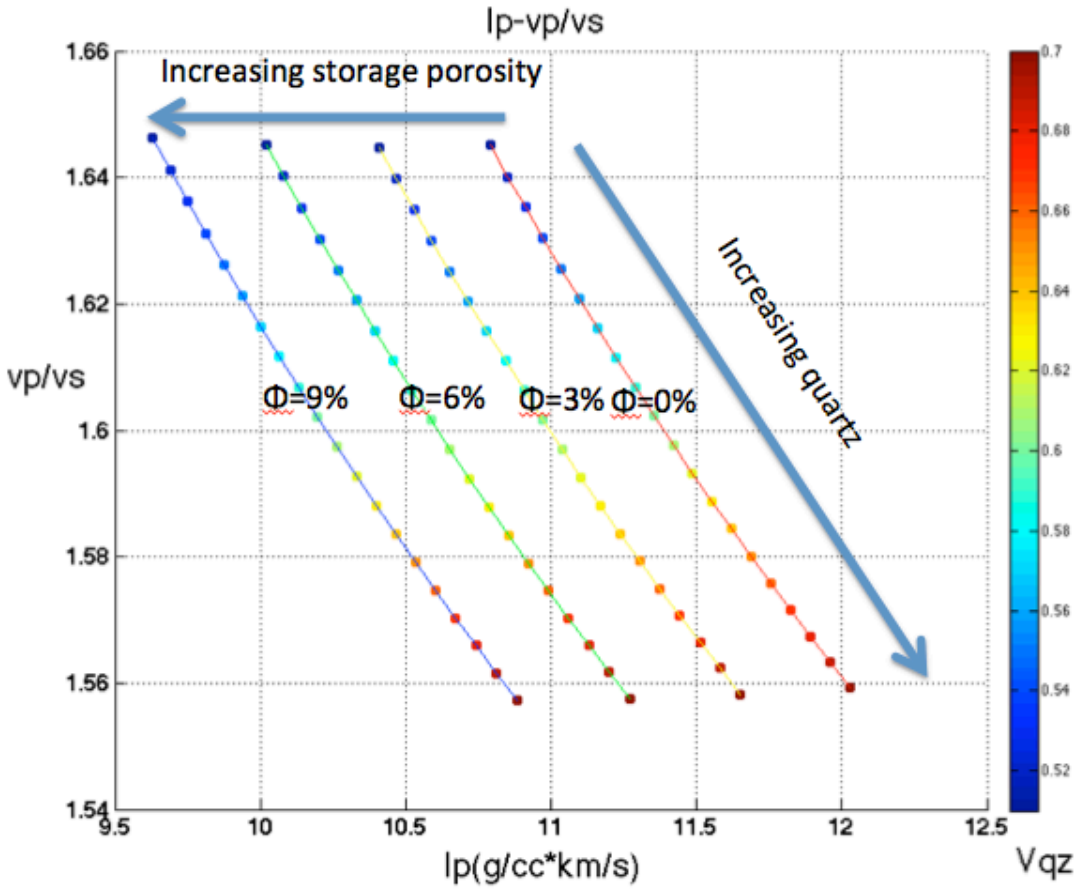

Figure 3-11 Cross-plot of P-wave impedance and Vp/Vs ratio. Assume 10% kerogen, 100% water saturation. As quartz increase from 50% to 70%, the Vp/Vs ratio decreased while the Ip increased. And as the porosity increase from 0% to 9%(Stiff pore, aspect ratio = 0.4), the Ip decreased while no obvious change on Vp/Vs.

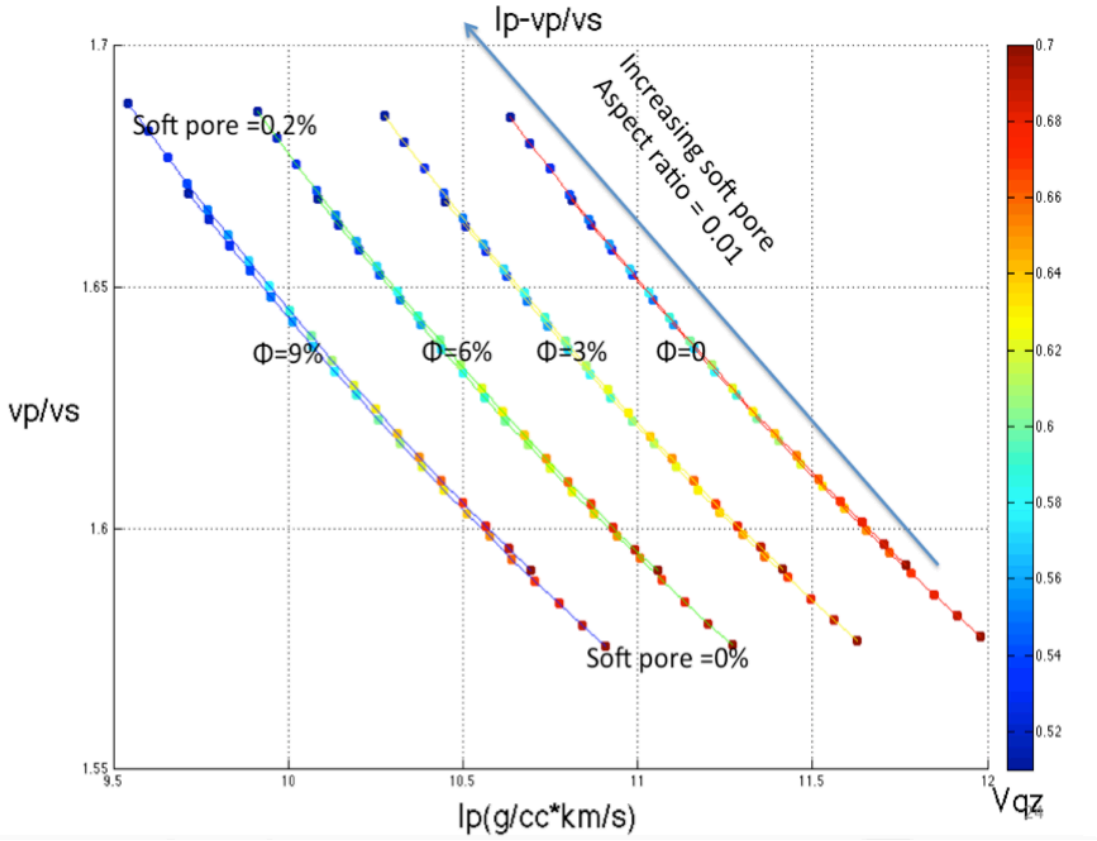

Figure 3-12 Cross-plot of P-wave impedance and Vp/Vs ratio. As soft pore increase from 0% to 0.2%, it increases vp/vs and decreases Ip.

Figure 3-12 shows soft pore has more influence on Ip and Vp/Vs compared with stiff pore. When the percentage of soft pore change form 0% to 0. 2%, it decreases Ip and increases Vp/Vs. This is because compared with stiffer pores soft pores have smaller aspect ratio therefore more compliant under pressures parallel to its short axis.

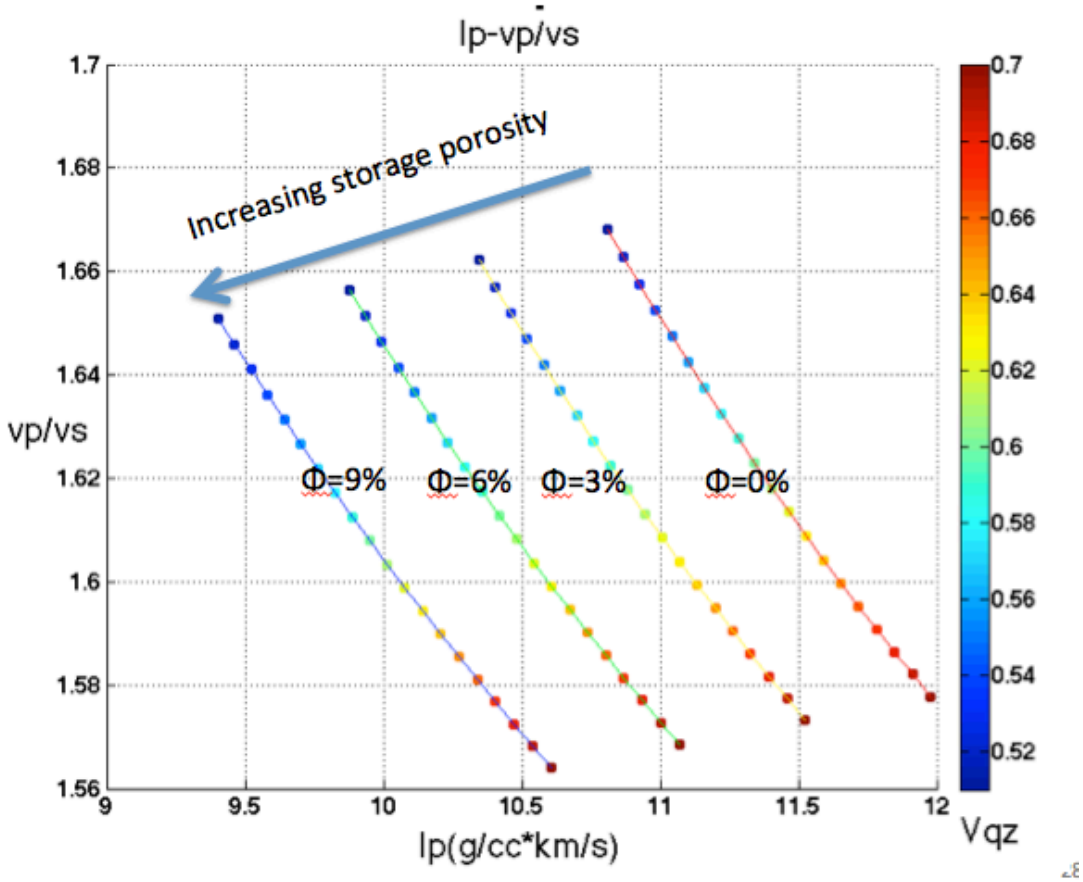

Figure 3-13 Cross-plot of P-wave impedance and Vp/Vs ratio for gas-saurated condition. As stiff pore increase from 0% to 9%, it decrease both Ip and Vp/Vs.

For gas-saturated condition, both Ip and Vp/Vs decrease with increasing porosity (aspect ratio = 0.4).

In summary, I find that

(1): In a rock system with clay-quartz mineralogy, increasing quartz content decreases the Vp/Vs ratio and increases the P-wave impedance. This is because quartz has relatively lower Vp/Vs and higher Ip compared with clay and kerogen.

(2): Increasing porosity decreases both the density and P-wave velocity, which results in the decreasing P-wave impedance. Increasing porosity should also increase Vp/Vs.

However, since the porosity here only increased form 0% to 9%, this effect is not obvious in Figure 3-12. Vp/Vs will show distinct increase if porosity increase from 0% to 40%.

(3): Soft pores have much stronger impact on Vp/Vs and Ip compared with stiff pores because they have much smaller bulk modulus compared with stiff pores.

(4): Compare Figure 4-11 and Figure 4-13, we can see that replace the fluid saturation from water (or oil) to gas will decrease both Ip and Vp/Vs.

So when we perform rock physics modeling, we need to consider the effects of mineralogy, porosity, pore shape and saturation fluid.

Chapter 4 Geophysical response of Barnett shale

4.1 Optimum seismic attribute for Barnett shale

Because of varying mineralogy, the Ip and Vp/Vs are not equally efficient for all shale reservoirs. For some shale formations, Ip is a more sensitive kerogen identification attributes while for others Vp/Vs is the more sensitive one. So what is the 'right' seismic attribute for Barnett shale?

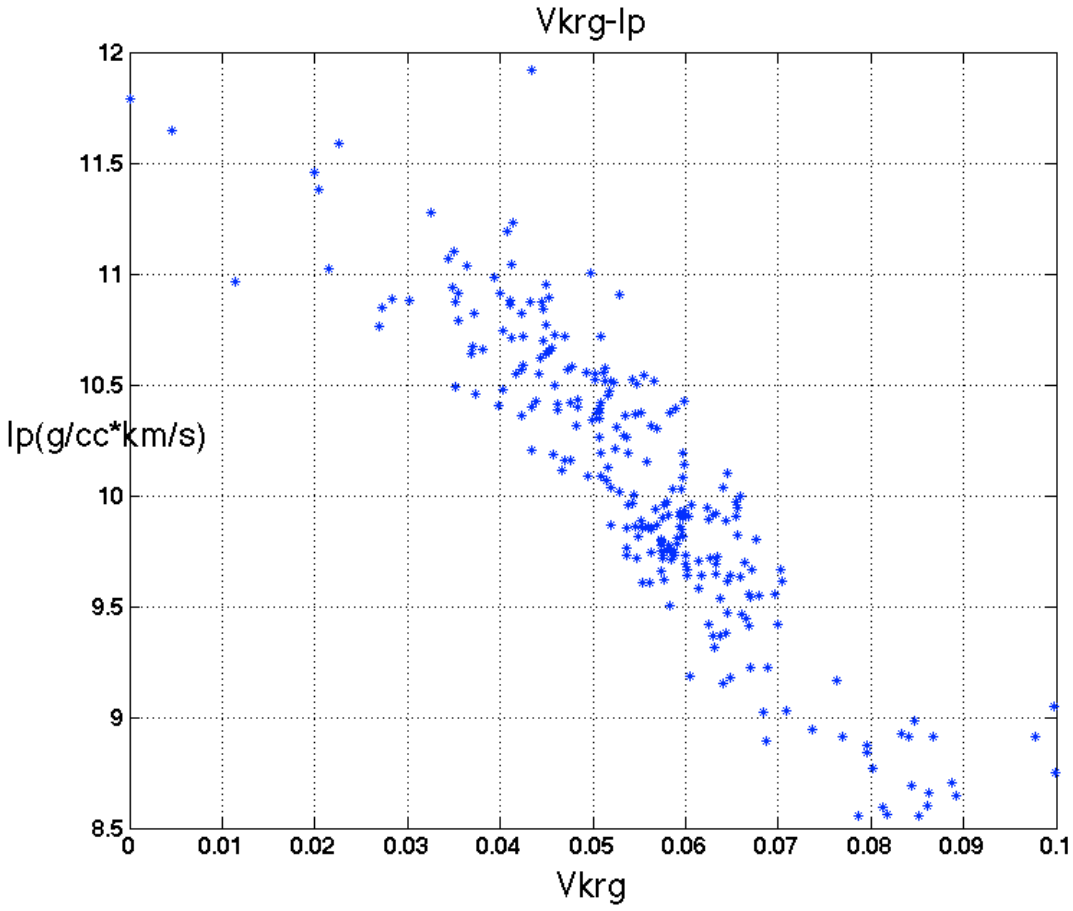

Figure 4-1 Relationship between P-wave impedance and the volume concentration of kerogen. P-wave impedance decrease as kerogen content increase. Data obtained in wells in Barnett shale.

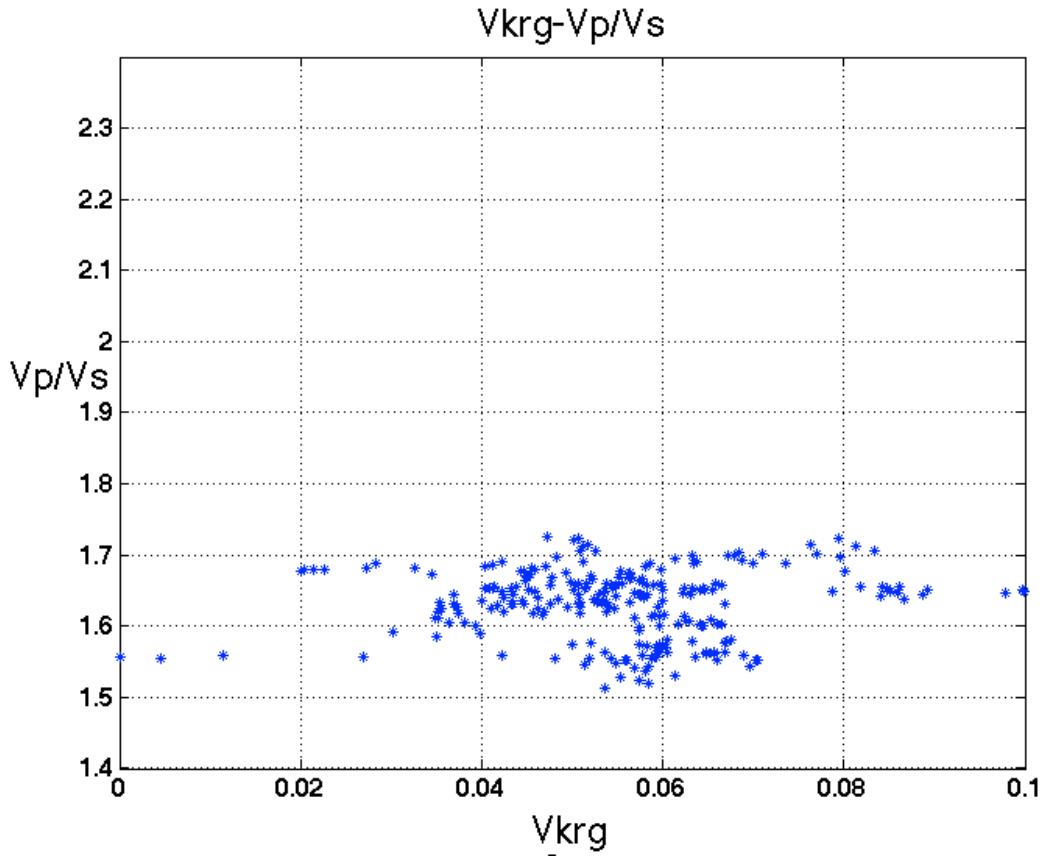

Figure 4-2 Relationship between Vp/Vs ratio and the volume concentration of kerogen. There is no clear changing trend for Vp/Vs when kerogen content increase. Data obtained in wells in Barnett shale.

Figures 4-1 and 4-2 show Barnett shale's Ip and Vp/Vs response on increasing kerogen content. We can see that P-wave impedance decreases with increasing kerogen content; and for Vp/Vs ratio, no clear trend can be observed. So for Barnett shale, Ip is a better kerogen identification attribute than Vp/Vs.

My explanation for this phenomenon is that, the Ip of kerogen is the lowest among kerogen, clay, quartz, and calcite, while the Vp/Vs of kerogen is higher than (or comparable to) quartz. This means if any Vp/Vs decrease is observed, it may be caused by either increasing quartz or increasing kerogen.

Ternary plot Figure 4-3 shows detailed mineral composition of Barnett shale. We can

see that quartz content changing within the range from 40% to 85%. This widely changing quartz content contaminates the Vp/Vs response of Barnett shale. In contrast, the quartz content of the clay-rich shale is constrained within a narrow range. Without the interference of changing quartz content, we may expect it to has a better Vp/Vs response.

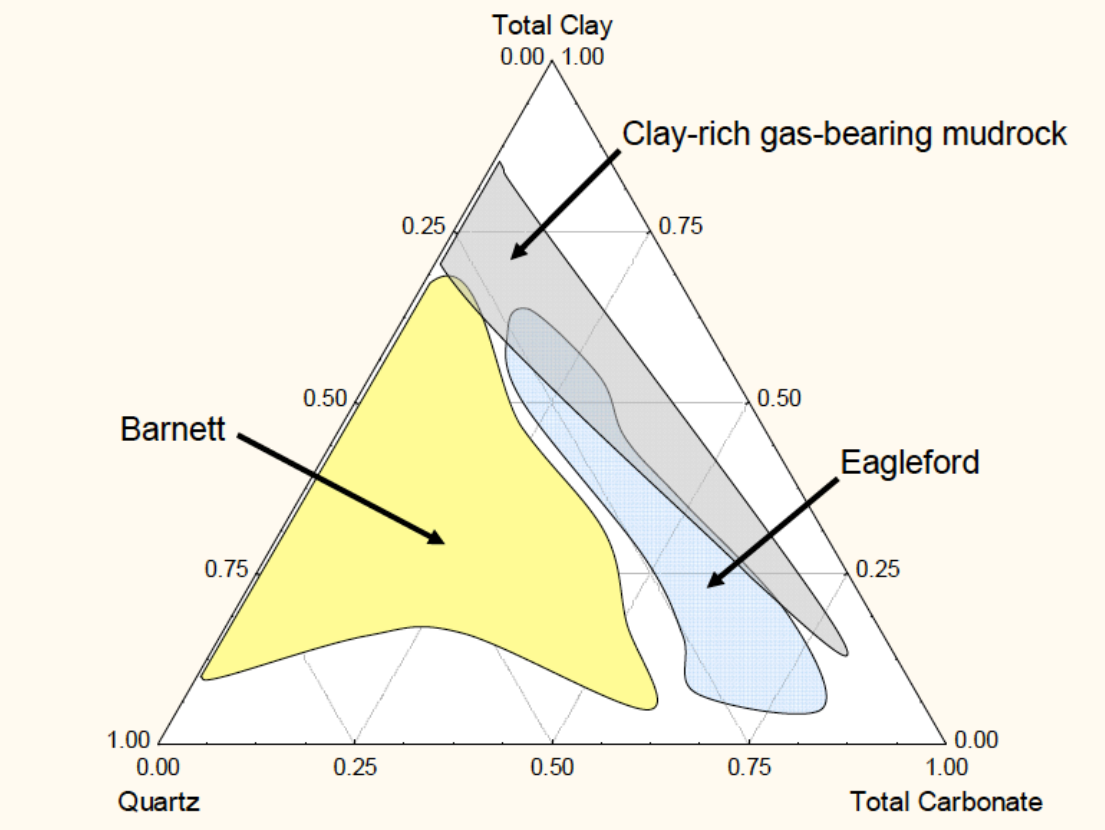

Figure 4-3 Ternary plot shows the mineral compositon of Barnett, Eagleford and other clay-rich shale (Passey et al., 2010)

Well log data (Figure 4-4) shows the detailed mineral composition of Barnett shale. We can see that within the Barnett shale, calcite volume percentage is relatively low except for several layers of spikes. Some layers are relatively clay-rich, while others are relatively quartz-rich.

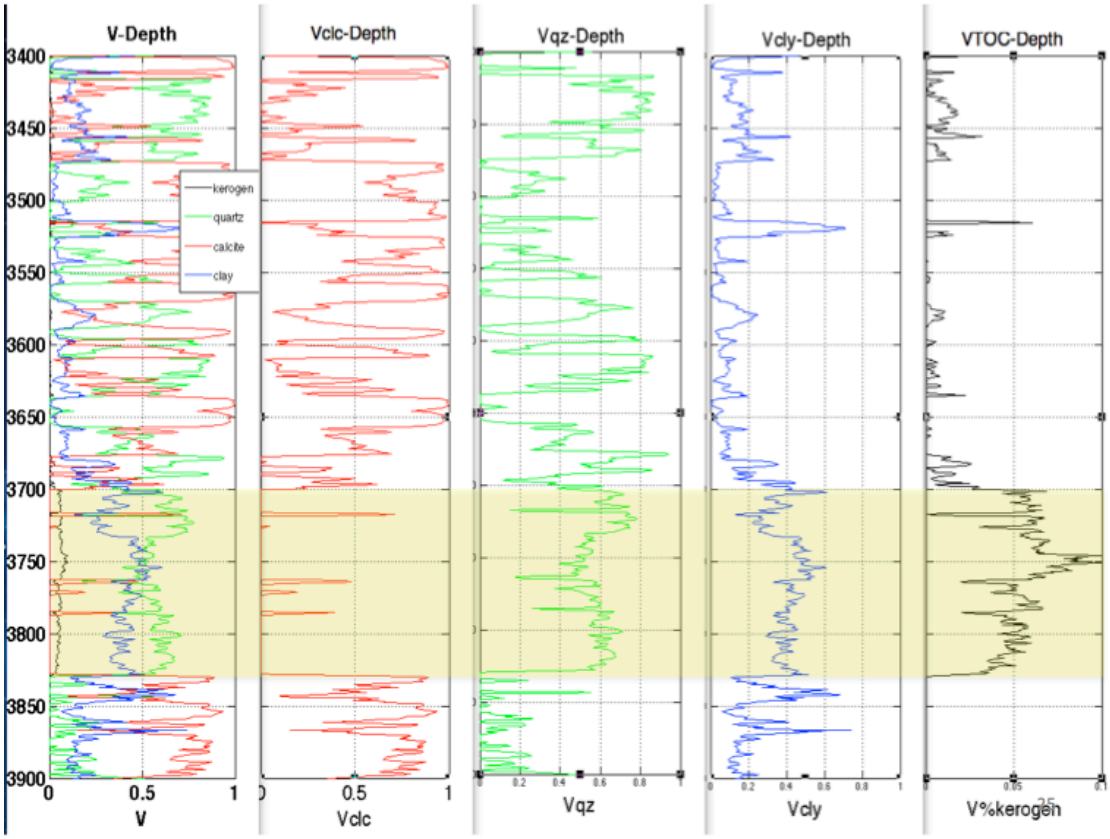

Figure 4-4 Well log data shows the normalized volume concentration of calciate, quartz, clay and kerogen of barnett shale (highed by yellow band). Other minor minerals are not considered here

To display the relationship between organic matter and the three minerals, I plot mineral composition ternary plot (Figure 4-5). Different colors are used to display the volume concentration of kerogen as shown in legend.

We can see that kerogen content decreases with increasing calcite content, and the mineralogy is mainly the quartz-clay mixture. Based on this I exclude all data points with high calcite content （calcite volume >20%）in the following analysis and set the mineralogy of the rock physics model as a quartz—clay mixture.

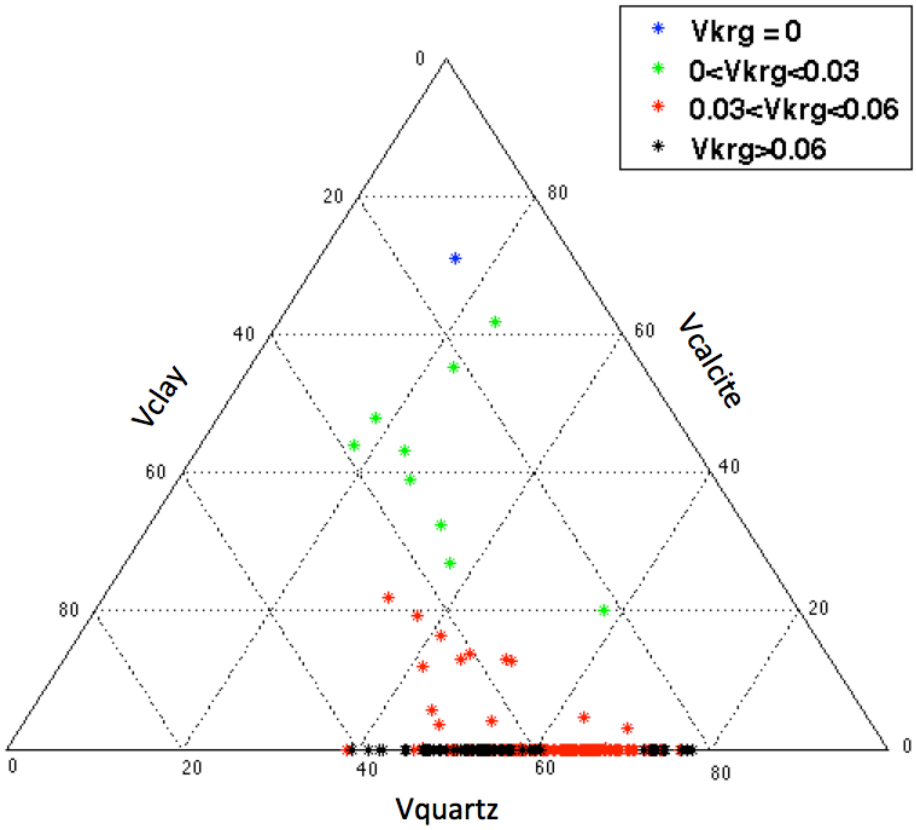

Figure 4-5 Mineral composition ternary plot for Barnett shale

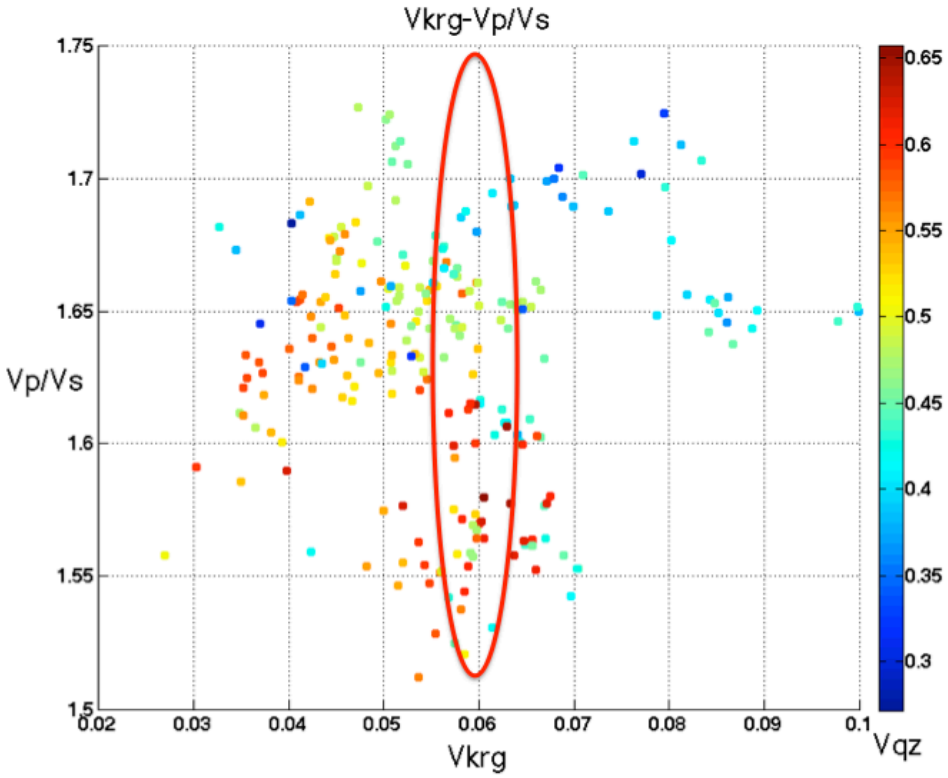

Figure 4-6 Relationship between kerogen content and Vp/Vs. Only those data points with calcite content lower than 20% are plotted here

I replot the Vp/Vs—kerogen content relationship (Figure 4-6) with a detailed scale, where the volume percentage of quartz is represented by color. We can see that even for the same TOC content, the Vp/Vs can span a wide range. Low Vp/Vs corresponds to high quartz content while high Vp/Vs corresponds to low quartz content. This confirms the previous statement that changing quartz content interfere the normal Vp/Vs response of kerogen.

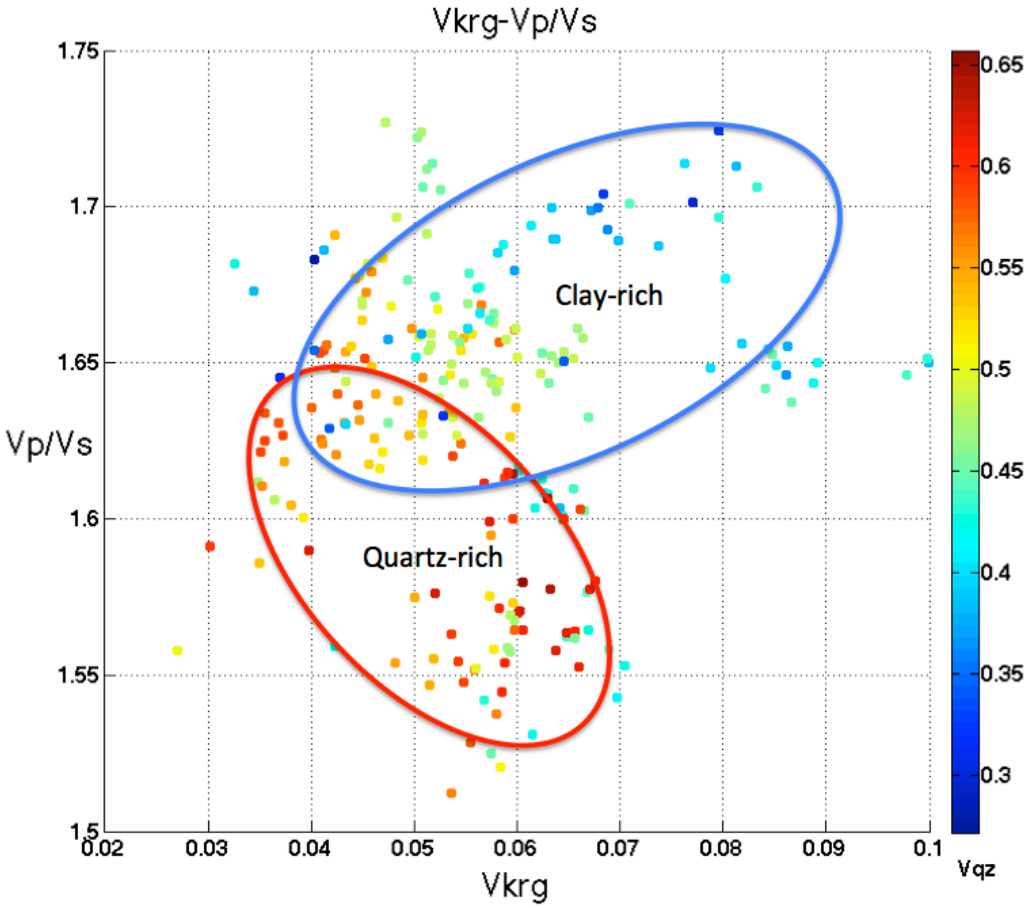

Figure 4-7 Relationship between kerogen content and Vp/Vs. For clay-rich data points, Vp/Vs increase with increasing kerogen volume. For quartz-rich data points, Vp/Vs decreases with increasing kerogen volume

Figure 4-6 also shows two distinct trends: For clay-rich data points, Vp/Vs increases with increasing kerogen volume. For quartz-rich data points, Vp/Vs decreases with

increasing kerogen volume (Figure 4-7). This observation reveals the possibility of using Vp/Vs as kerogen content indicator for quartz-rich data and clay-rich data respectively.

4.2 Rock physics modeling for Barnett shale

To predict the geophysical response from in-situ rock parameters, I separate the rock physics model into clay-rich model and quartz-rich model. I will first discuss the clay-rich model.

Clay-rich model

In-situ rock parameters like mineral composition, porosity, and saturation etc. are needed for the rock physics modeling of clay-rich layers in Barnett shale.

As shown in Figure 4-8, the relationship between porosity and kerogen content is obtained using a first-order polynomial fit. And the result shows:

$$\Phi = 0.9328 * Vkerogen + 0.03878$$

The mineralogy of clay-rich layers (quartz % < 38%) can be expressed by kerogen content (Figure 4-9):

$$Vclay = 1.044 * Vkerogen + 0.3525$$

The velocity of carrying fluid controls the deposited particle size of detrital sedimentary rocks. The preservation of organic matter, which require low oxygen environment, is also partially controlled by the fluid velocity. Fast moving stream is more disturbed therefore have more oxygen, while quiet water is less disturbed therefore its bottom deposition layer has less oxygen. So the quiet water environments

which deposit clay particles is also friendly to the preservation of organic matter. This is why kerogen content increases with increasing clay volume content.

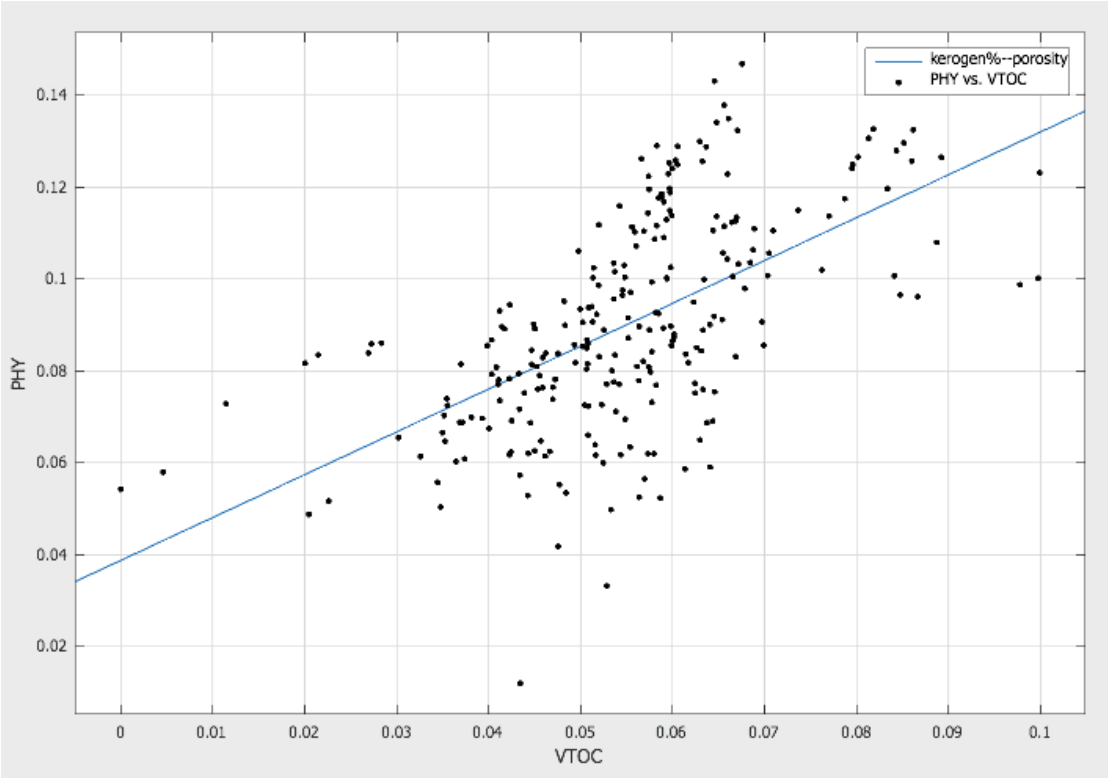

Results

Linear model Poly1:
f(x) = p1*x + p2
Coefficients (with 95% confidence bounds):
p1 = 0.9328 (0.7742, 1.091)
p2 = 0.03878 (0.02974, 0.04782)

Goodness of fit:
SSE: 0.08517
R-square: 0.3532
Adjusted R-square: 0.3506
RMSE: 0.01861

Figure 4-8 First-order polynomial fit for the relationship between kerogen content and porosity. Porosity increases with increasing kerogen content.

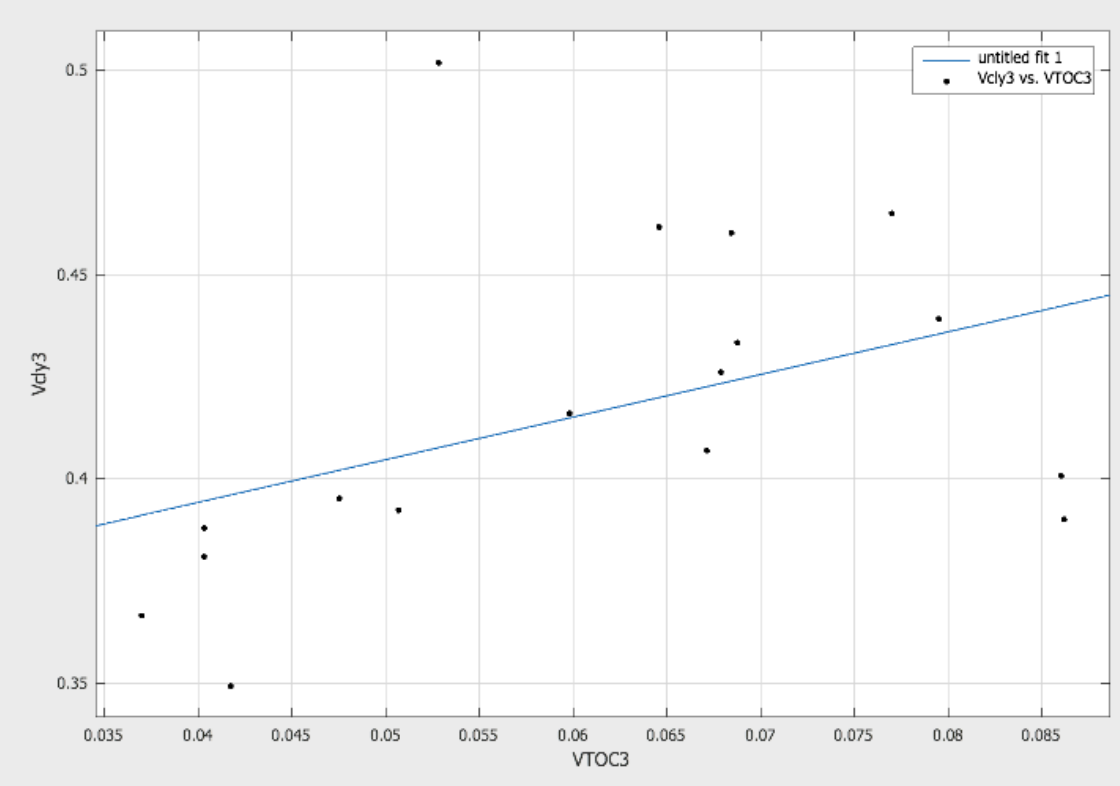

Results

Linear model Poly1:
f(x) = p1*x + p2
Coefficients (with 95% confidence bounds):
p1 = 1.044 (-0.182, 2.271)
p2 = 0.3525 (0.2753, 0.4296)

Goodness of fit:
SSE: 0.02101
R-square: 0.1801
Adjusted R-square: 0.1254
RMSE: 0.03743

Figure 4-9 First-order polynomial fit for the relationship between kerogen content and clay content. Kerogen content increases with increasing clay content.

Take the $\Phi - Vkerogen$ and *Vclay -- Vkerogen* relationship into account; the model predicted Ip-vp/vs cross-plot calculated by SCA method is shown in Figure 4-11. The fluid saturation inputs are the averaged value within clay-rich layers for gas, water, and oil respectively (Figure 4-10). The volume of water saturation was added to clay

volume percentage; and wet clay bulk and shear moduli value are used as input data (K = 25Gpa, MU = 9Gpa). The bulk and shear moduli of oil-gas mixture are calculated by Reuss bound; then this mixture is directly treated as inclusion when performing SCA method.

The fraction of stiff pore in total porosity is assumed as 0.7.

We can see that according to model prediction Figure 4-11, Ip decreases with increasing kerogen content while Vp/Vs increases with increasing kerogen content. This conflicts with the previous conclusion that increasing kerogen decreases both Ip and Vp/Vs (section 3.2). The explanation is when kerogen increases, clay increases at the same time. So, it's the increasing clay that increases the Vp/Vs.

The well log data agrees with the model prediction quite well (Figure 4-12).

The thin section Figure 4-13 shows that quartz grains suspended in a clay matrix. This means clay should have more contribution to the effective elastic property of the whole rock.

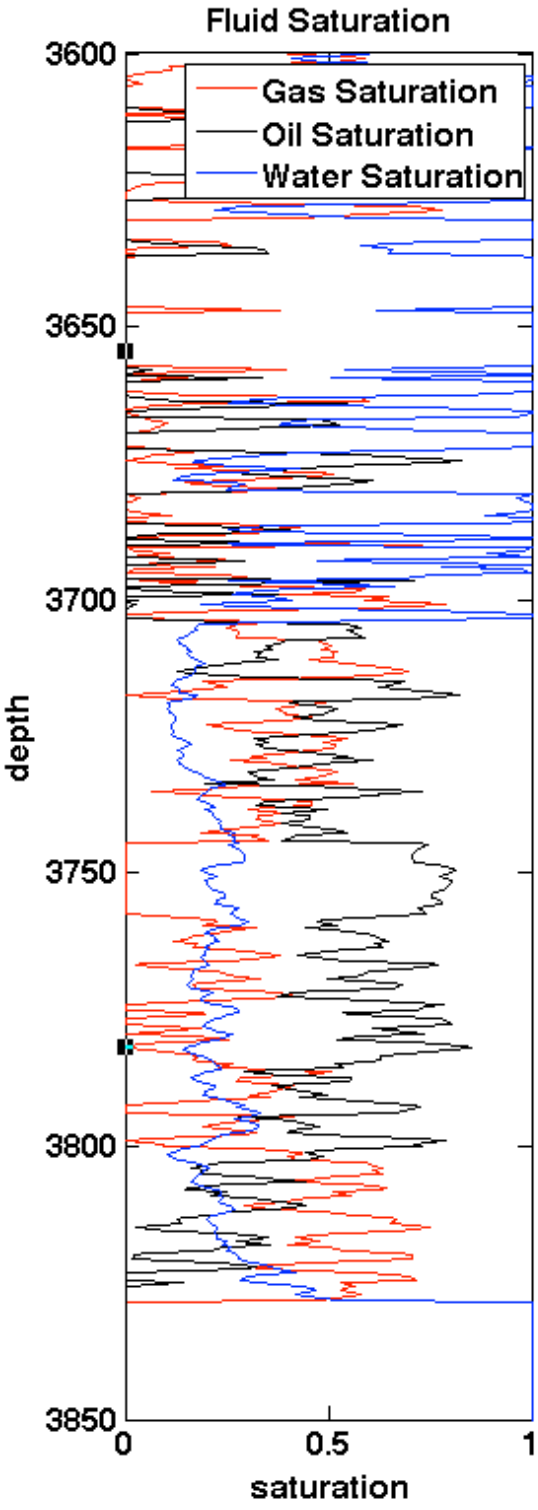

Figure 4-10 Fluid saturation for Barnett shale

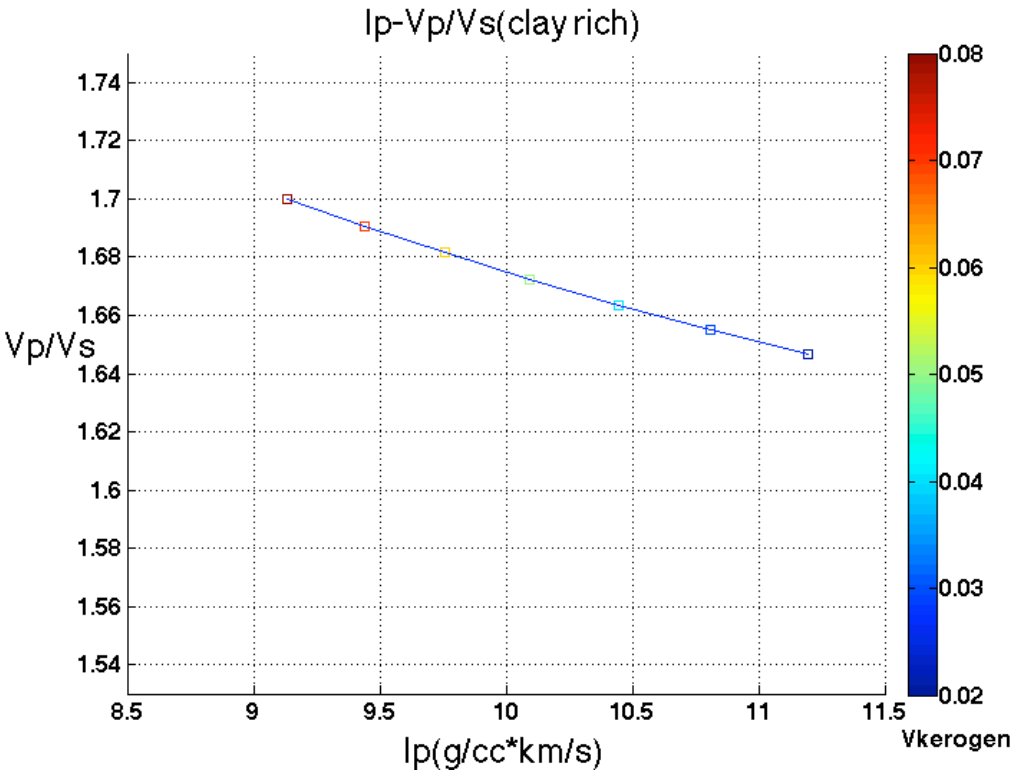

Figure 4-11 Model predict Ip-Vp/Vs cross-plot for clay-rich condition

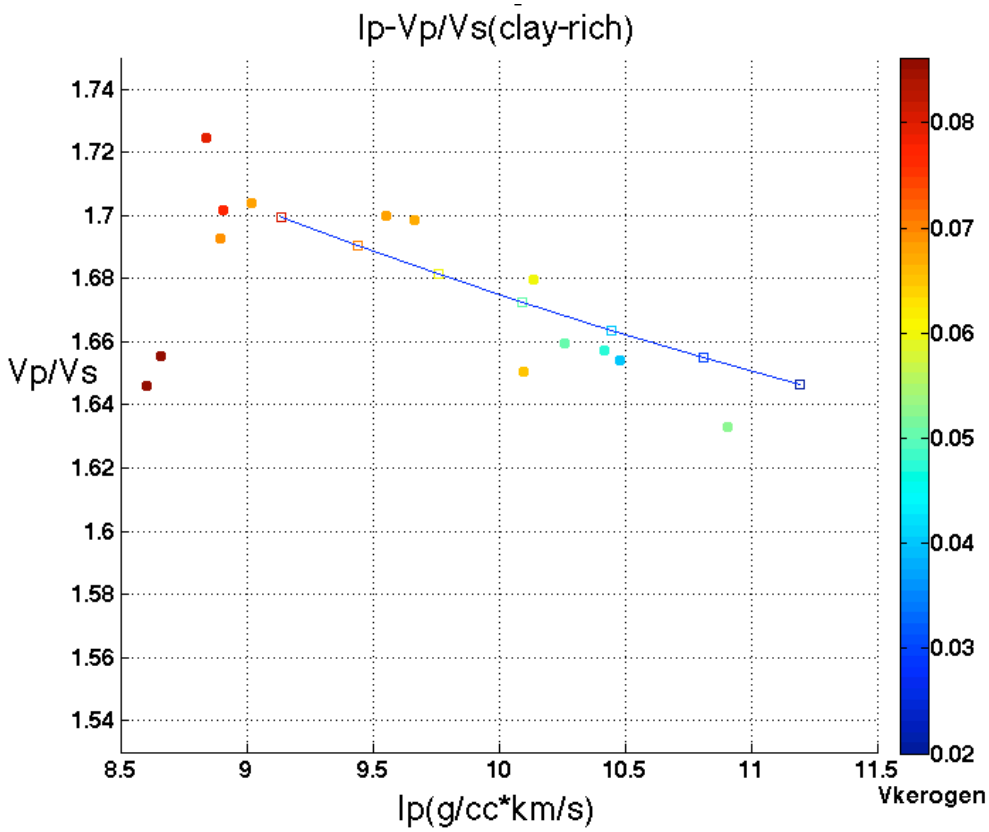

Figure 4-12 Model predicted Ip-Vp/Vs crossplot with well log data for clay-rich condition

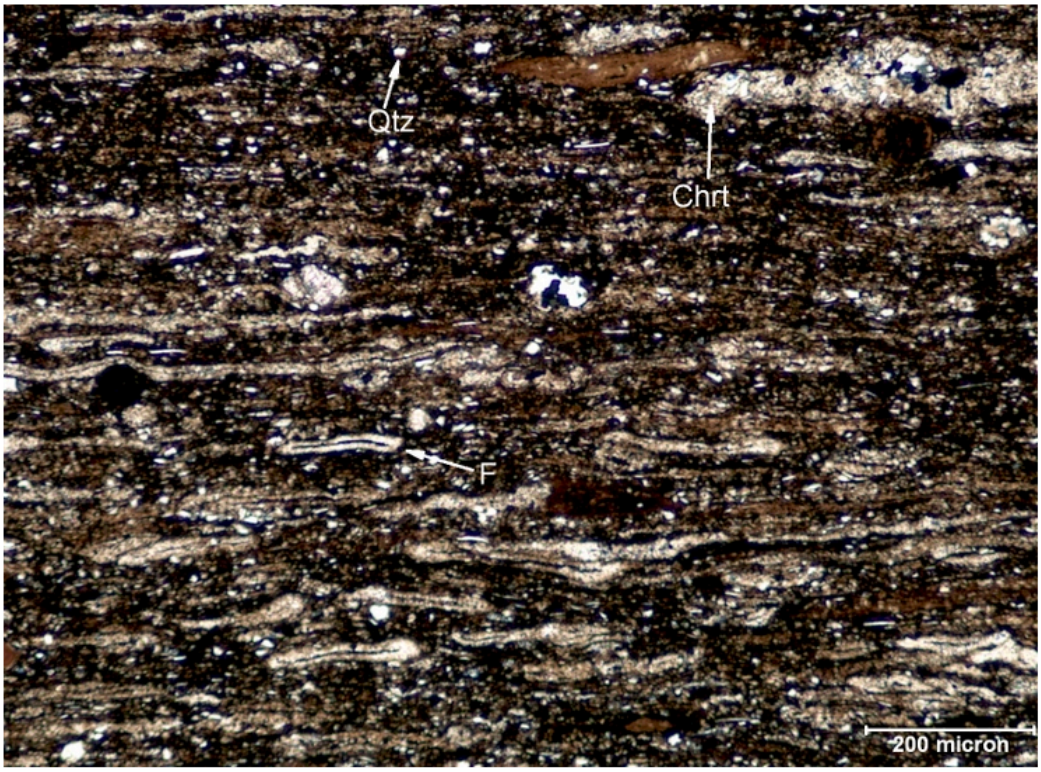

Figure 4-13 Thin section of core sample from clay-rich layers

Quartz-rich model

For quartz-rich condition (quartz% > 58%), the relationship between quartz content and kerogen content is obtained by first-order polynomial fit (Figure 4-14), which is:

$$Vquartz = 0.8665 * Vkerogen + 0.5584$$

The model predicted Ip-Vp/Vs cross-plot is shown in Figure 4-15. We can see that according to model prediction, both Ip and Vp/Vs decrease with increasing kerogen content. This is because both kerogen and quartz has low Vp/Vs. The well log data agrees with the model prediction quite well (Figure 4-16).

The thin section Figure 4-17 shows that quartz grains begin to have some contact with each other. Which means quartz will have more effect on the effective elastic property

compared with the previous suspension condition.

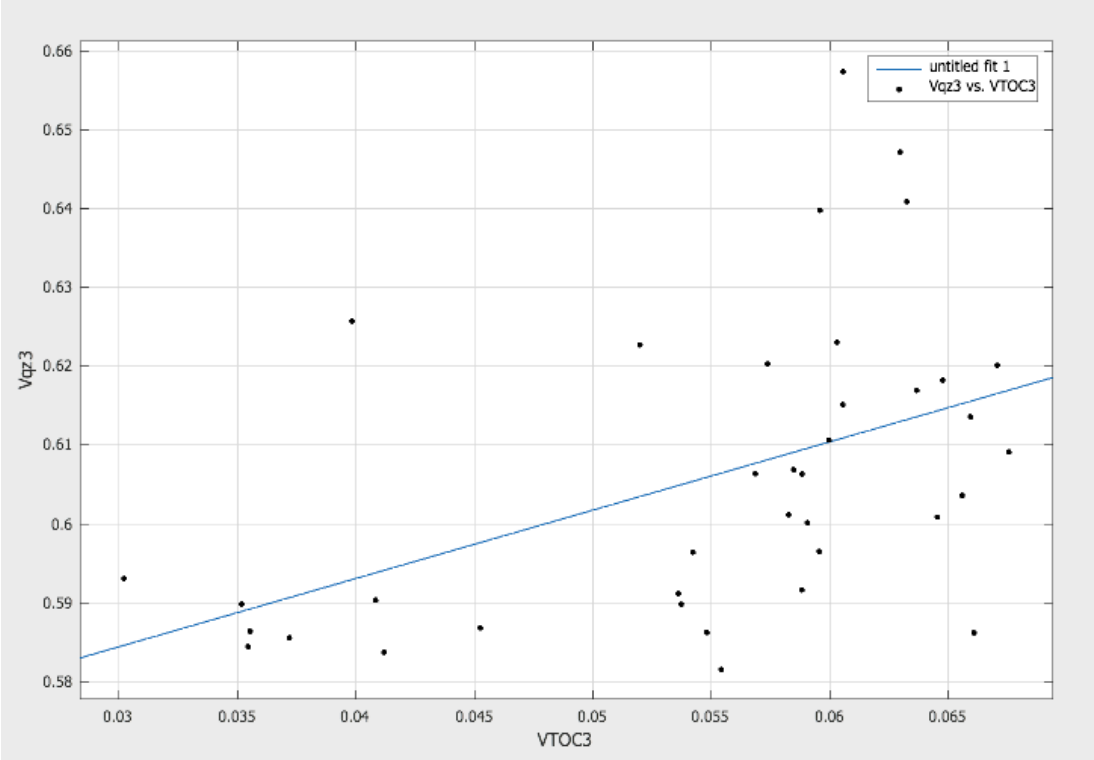

Results

Linear model Poly1:
f(x) = p1*x + p2
Coefficients (with 95% confidence bounds):
p1 = 0.8665 (0.3238, 1.409)
p2 = 0.5584 (0.5281, 0.5887)

Goodness of fit:
SSE: 0.01057
R-square: 0.2256
Adjusted R-square: 0.2041
RMSE: 0.01714

Figure 4-14 First-order polynomial fit for the relationship between kerogen content and quartz content. Kerogen content increases with increasing quartz content.

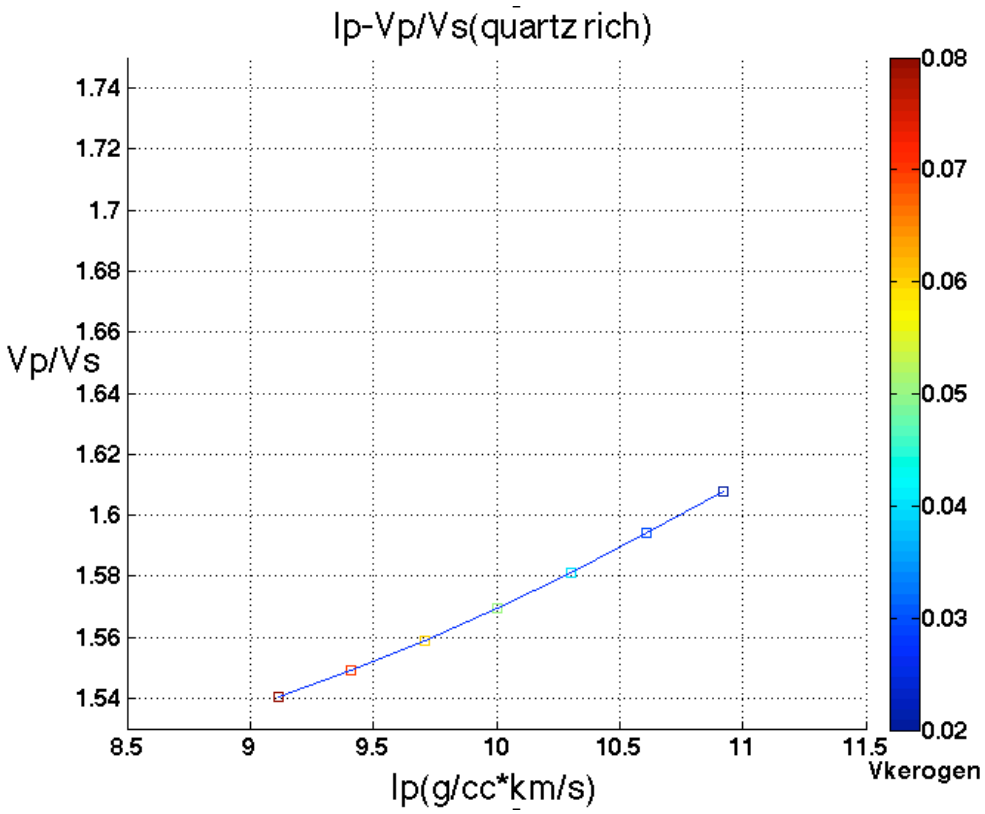

Figure 4-15 Model predict Ip-Vp/Vs cross-plot for quartz-rich condition

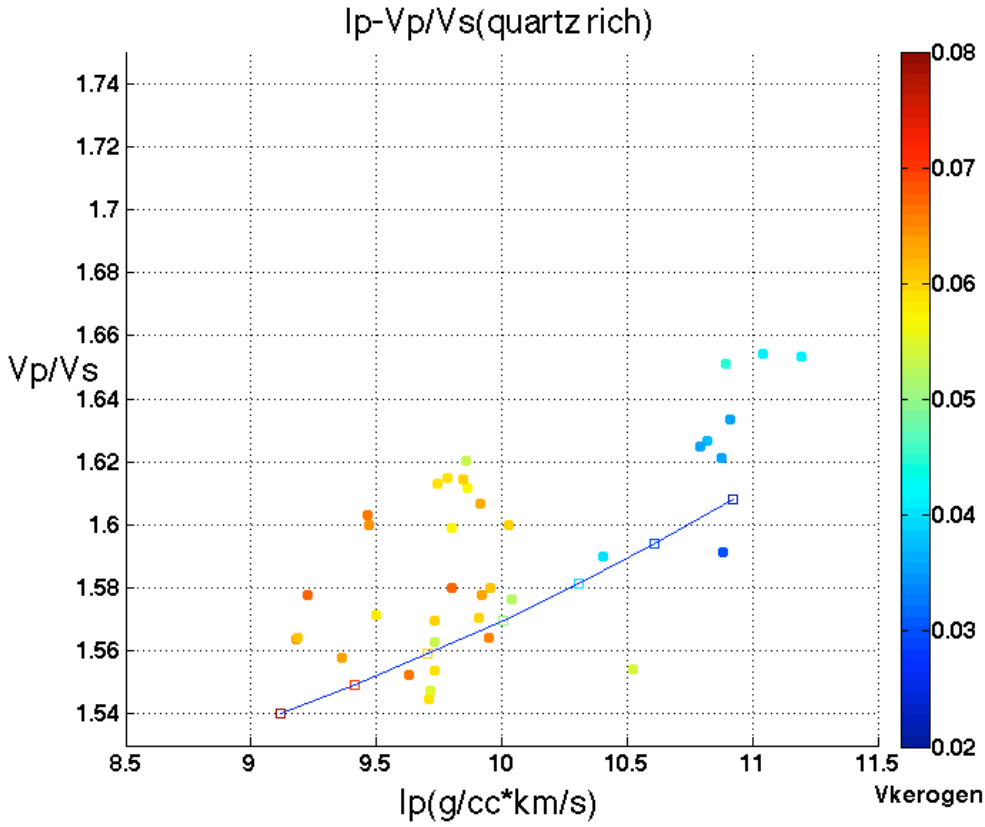

Figure 4-16 Model predicted Ip-Vp/Vs crossplot with well log data for quartz-rich condition

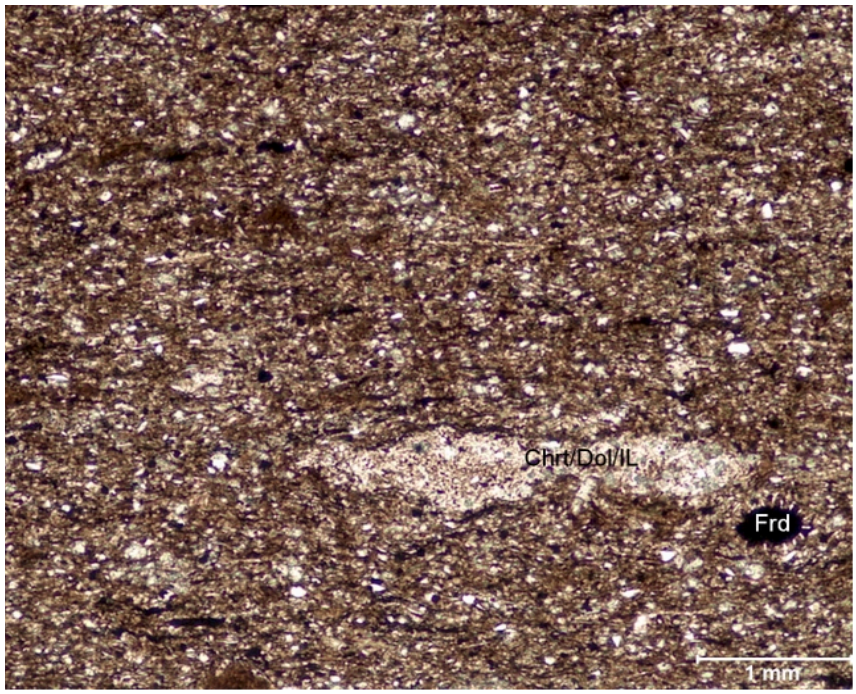

Figure 4-17 Thin section of core sample from quartz-rich layers

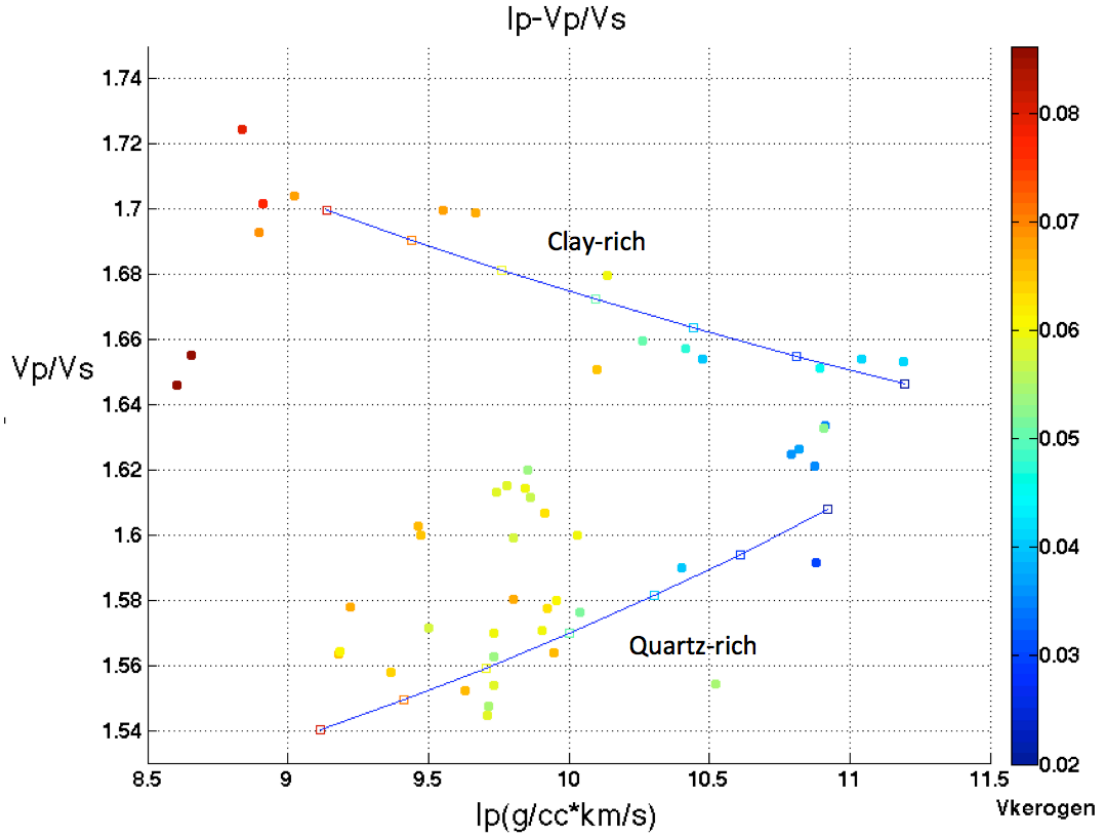

Figure 4-18 Model predicted Ip-Vp/Vs crossplot with well log data for quartz-rich and clay-rich condition

By plotting the quartz-rich and clay-rich condition together in Figure 4-18, we can see that clay rich layers have higher TOC concentrations, higher Vp/Vs and lower Ip compared with quartz-rich layers.

For production purpose, we usually prefer the quartz-rich layers. Though it has less kerogen content, it is more brittle and hydraulic fracturing can be performed more easily.

Chapter 5 Summary and Discussion

Using rock physics modeling, I have studied the effects of kerogen, mineralogy, porosity, pore shape, and saturation on the seismic attributes impedance and Vp/Vs. For a clay-kerogen system, the effective Ip and Vp/Vs decrease with increasing kerogen content. For a clay-quartz system, the effective Ip increases with increasing quartz content and the effective Vp/Vs decreases with increasing quartz content. The effect of increasing water (or oil) filled porosity is to decreases Ip. Decreasing the aspect ratio of pores increases Vp/Vs and decreases Ip. Replacing the fluid saturation from water (or oil) to gas decreases both Ip and Vp/Vs.

The effects of mineralogy have been discussed in detail in section 4. The geophysical response of shale reservoir is affected by its average mineral composition. Different average mineral composition of two shale reservoirs may result in different behaviors of their geophysical response; while similar average mineral composition may cause their geophysical response to behave similarly. For those shale reservoirs have clay-shale mixture mineralogy, like Barnett, Ip is generally a better kerogen identification attribute than Vp/Vs. This is because the Ip of kerogen is the lowest among kerogen, clay, quartz, and calcite, while the Vp/Vs of kerogen is higher than quartz. If quartz content varies widely within the individual shale play, either increasing quartz or increasing kerogen may cause decrease of Vp/Vs. So the randomly changing quartz content may seriously contaminate the Vp/Vs response on

kerogen content.

Observation of Barnett shale data shows

1: Kerogen volume content, which has positive correlation with porosity, is the dominant parameter to reduce P-wave impedance.

2: Kerogen content seems positively correlate to high clay content (which increase the Vp/Vs to 1.7) or high quartz content (which decrease the Vp/Vs to 1.54); and it is negatively correlate to high calcite content.

These observations are consistent with the following mineral properties:

1: Layered (cracked), porous Kerogen with hydrocarbon saturation (oil and gas) has a very low modulus and low vertical Vp/Vs ratio.

2: Compacted, water-saturated clay have lower moduli but higher Vp/Vs compared with quartz. It will dominate the property of clay-dominant rocks.

3: Quartz-rich organic shale has higher moduli and lower Vp/Vs. It maybe an ideal reservoir rock since it is more brittle compared with clay-dominated shale.

My future work includes:

1: Test the above conclusions with more well log datas (Barnett and other shale formations).

2: Invert the in-situ rock parameters from seismic data.

3: Take into account the effects of anisotropy.

REFERENCES

Bartis, J. T., LaTourrette, T., Dixon, L., Peterson, D.J., Cecchine, G., 2005. Oil Shale Development in the United States. Prospects and Policy Issues. Prepared for the National Energy Technology Laboratory of the United States Department of Energy. The RAND Corporation. ISBN 978-0-8330-3848-7. Retrieved 2007-06-29.

Beers, R. F., 1945. Radioactivity and organic content of some Paleozoic shales. AAPG Bulletin, 29(1), 1-22.

Berryman, J. G., 1980. Long wavelength propagation in composite elastic media I. Spherical inclusions. The Journal of the Acoustical Society of America, 68, 1809-1819.

Berryman, J.G., 1995. Mixture theories for rock properties. In Rock Physics and Phase Relations: a Handbook of Physical Constants, ed. T.J. Ahrens. Washington, DC: American Geophysical Union, 205–228.

Budiansky, B., 1965. On the elastic moduli of some heterogeneous materials. J. Mech. Phys. Solids, 13, 223–227.

Bissada, A., 1994. Quantitative petroleum generation and migration analysis for play evaluation and prospect ranking. Course notes. Department of Geosciences, University of Houston.

Fertl, W.H., and H.H. Rieke., 1980. Gamma-ray spectral evaluation techniques identify fractured shale reservoirs and source-rock characteristics: Journal of Petroleum Technology. 31, 2053-2062.

Han, D. H., 1986. Effects of porosity and clay content on acoustic properties of sandstones and unconsolidated sediments. PhD Dissertation. Stanford Univ., CA (USA).

Hill, R., 1965. A self-consistent mechanics of composite materials. J. Mech. Phys. Solids, 13, 213–222.

International Energy Agency (IEA) website

Lee, Sunggyu., Speight, James G., Loyalka, Sudarshan K., 2007. Handbook of Alternative Fuel Technologies. CRC Press. p. 290. ISBN 978-0-8247-4069-6. Retrieved 2009-03-14.

Mavko, G., Mukerji, T., & Dvorkin, J., 2009. The Rock Physics Handbook, second edition, Tools for Seismic Analysis in Porous Media. Cambridge University Press.

Meissner.F.F., 1978. Petroleum geology of the Bakken Formation Williston Basin, North Dakota and Montana, in The Economic Geology of the Williston Basin: Montana Geological Society. 1978 Williston Basin Symposium. 207-227

Nixon, R.P., 1973. Oil source beds in Cretaceous Mowry Shale of northwestern interior United States: AAPG Bulletin, 57, 136-161

Passey, Q. R., Creaney, S., Kulla, J. B., Moretti, F. J., and Stroud, J. D., 1990. A practical model for organic-richness from porosity and resistivity logs. AAPG Bulletin, 74(12), 1777-1794.

Passey, Q., Bohacs, K., Esch, W., Klimentidis, R., and Sinha, S., 2010. June. From Oil-prone source rock to gas-producing shale reservoir-geologic and petrophysical characterization of unconventional shale gas reservoirs. In International Oil and Gas Conference and Exhibition in China.

Tarbuck, E.J, Lutgens, F.K., 2008. Earth—An introduction to physical geology, ninth edition. Macmillan Publishing Company.

Schmoker, J. W., 1981. Determination of organic-matter content of Appalachian Devonian shales from gamma-ray logs. AAPG Bulletin, 65(7), 1285-1298.

Schmoker, J. W., & Hester, T. C., 1983. Organic carbon in Bakken Formation, United States portion of Williston basin. AAPG Bulletin, 67(12), 2165-2174.

Schmoker, J. W., and T.C. Hester., 1989. Oil generation inferred from formation resistivity—Bakken Formation, Williston basin, North Dakota: Transactions of the Thirtieth SPWLA Annual Logging Symposium, Paper H.

Swanson, V. E., 1960. Oil yield and uranium content of black shales: USGS Professional Paper 356-A. 1-44

Supernaw, I.R., D.M. Arnold, and A.J. Link., 1978. Method for in-situ evaluation of the source rock potential of earth formations: United States Patent 4.071.744. January 31, 1978

Wu, T.T., 1966. The effect of inclusion shape on the elastic moduli of a two-phase material. Int. J. Solids Structures, 2, 1–8.

Zhu, Y., Liu, E., Martinez, A., Payne, M.A., Harris, C.E., 2011. Understanding geophysical response of shale-gas plays, The Leading Edge,30, 332-338.